

Automatic Perturbation Analysis on General Computational Graphs

Kaidi Xu^{1*}, Zhouxing Shi^{2*}, Huan Zhang^{3*}
Minlie Huang², Kai-Wei Chang³, Bhavya Kailkhura⁴, Xue Lin¹, Cho-Jui Hsieh³

¹Northeastern University ²Tsinghua University ³UCLA

⁴Lawrence Livermore National Laboratory (LLNL)

xu.kaid@husky.neu.edu, zhouxingshichn@gmail.com, huan@huan-zhang.com

aih Huang@tsinghua.edu.cn, kw@kwchang.net, kailkhura1@llnl.gov

xue.lin@northeastern.edu, chohsieh@cs.ucla.edu

Abstract

Linear relaxation based perturbation analysis for neural networks, which aims to compute tight linear bounds of output neurons given a certain amount of input perturbation, has become a core component in robustness verification and certified defense. However, the majority of linear relaxation based methods only consider feed-forward ReLU networks. While several works extended them to relatively complicated networks, they often need tedious manual derivations and implementation which are arduous and error-prone. Their limited flexibility makes it difficult to handle more complicated tasks. In this paper, we take a significant leap by developing an *automatic perturbation analysis* algorithm to enable perturbation analysis on any neural network structure, and its computation can be done automatically in a similar manner as the back-propagation algorithm for gradient computation. The main idea is to express a network as a computational graph and then generalize linear relaxation algorithms such as CROWN as a graph algorithm. Our algorithm itself is differentiable and integrated with PyTorch, which allows to optimize network parameters to reshape bounds into desired specifications, enabling automatic robustness verification and certified defense. In particular, we demonstrate a few tasks that are not easily achievable without an automatic framework. We first perform certified robust training and robustness verification for complex natural language models which could be challenging with manual derivation and implementation. We further show that our algorithm can be used for tasks beyond certified defense – we create a neural network with a *provably* flat optimization landscape and study its generalization capability, and we show that this network can preserve accuracy better after aggressive weight quantization. Code is available at https://github.com/KaidiXu/auto_LiRPA.

1 Introduction

Deep Neural Networks (DNNs) are powerful functional approximators, but they can be highly non-convex and non-linear, making it challenging to study and understand their behaviors. One fundamental tool to studying the behavior of such non-linear systems is *perturbation analysis*: given a certain amount of perturbation on an input variable, the goal is to approximate or find upper and lower bounds of outputs. Intuitively, to understand how perturbations affect the output of a DNN f , one simple way is to take the gradient with respect to some network variable \mathbf{x} , and $\nabla_{\mathbf{x}}f(\mathbf{x})$ provides some clues on how f near point \mathbf{x} behaves by forming a linear approximation $f(\mathbf{x} + \delta) \approx f(\mathbf{x}) + \delta^T \nabla_{\mathbf{x}}f(\mathbf{x})$. However, this is only correct when $\delta \rightarrow 0$, and more importantly, it cannot provide certified bounds for output neurons.

To deploy DNN based models to critical applications such as aircraft control, autonomous driving and security cameras, it is crucial to test whether the behavior of a DNN model is provably consistent with certain user-specified properties, such as robustness, safety or reachability (Katz et al., 2017; Julian et al., 2019). A

*Equal Contribution

stronger type of perturbation analysis which gives guaranteed lower and upper bound of $f(\mathbf{x} + \delta)$ is necessary. Unfortunately, finding the tightest upper and lower bounds of output neurons is NP-complete for a fully connected ReLU network (Katz et al., 2017).

To get relatively tight upper and lower bounds of output neurons while being computationally feasible, many closely related works has been proposed recently (Wong & Kolter, 2018a; Zhang et al., 2018; Weng et al., 2018; Singh et al., 2018; Wang et al., 2018b; Singh et al., 2019b). The main idea is to give linear upper and lower bounds for output neurons w.r.t. the input under perturbation: $\underline{f}(\mathbf{x}_0 + \delta) \leq f(\mathbf{x}_0 + \delta) \leq \overline{f}(\mathbf{x}_0 + \delta)$ for some constrained δ , where $\overline{f}(\mathbf{x}_0 + \delta) := \overline{\mathbf{A}}(\mathbf{x}_0 + \delta) + \overline{\mathbf{b}}$ and $\underline{f}(\mathbf{x}_0 + \delta) := \underline{\mathbf{A}}(\mathbf{x}_0 + \delta) + \underline{\mathbf{b}}$ are two linear functions. We refer to this line of work as a **Linear Relaxation based Perturbation Analysis (LiRPA)** for short) for DNNs. Unlike the gradient based approximation, this method provides two hyperplanes that guarantee to cover $f(\mathbf{x}_0 + \delta)$, as illustrated in Figure 1. LiRPA has become a core component in applied to scenarios such as neural network robustness verification (Wang et al., 2018c; Zhang et al., 2018; Weng et al., 2018; Balunovic et al., 2019; Ko et al., 2019; Shi et al., 2020) and certified defense (Wong & Kolter, 2018a; Mirman et al., 2018; Wang et al., 2018a; Zhang et al., 2019a). Furthermore, LiRPA can serve as a general toolbox to understand the behavior of DNNs within a predefined input region, and can be used for interpretation and explanation of DNNs (Ko et al., 2019; Shi et al., 2020).

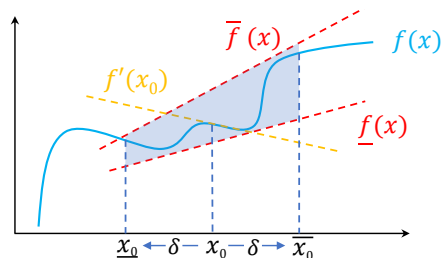


Figure 1: LiRPA bounding lines (red) vs. gradient based approximation (yellow) for a 1-D example. The approximation based on taking the gradient $f'(x_0)$ is inaccurate unless δ is extremely small and it cannot provide certified bounds. In contrast, LiRPA bounding lines provide certified upper and lower bound for $f(x)$, $x \in [x_0 - \delta, x_0 + \delta]$.

The majority development of LiRPA focused on feed-forward ReLU networks, but it is important to consider more complicated network structures and activations for real-world applications. To extend LiRPA beyond simple feed-forward networks, Wong et al. (2018) implemented it for ResNet on computer vision tasks; Zügner & Günnemann (2019) extended Wong & Kolter (2018a) to graph convolutional networks; Ko et al. (2019) and Shi et al. (2020) extended CROWN (Zhang et al., 2019a) to recurrent neural network and Transformers respectively. Unfortunately, many of these works require tedious manual derivation and implementation of these bounds for a specific network architecture. For example, Ko et al. (2019); Shi et al. (2020) both include more than 20 pages of derivations detailing the bounds for a specific model respectively. This severely restricts the applications of this perturbation analysis method, as bounds must be manually derived and implemented for any new network structures, which requires expert knowledge and tremendous implementation effort.

In this paper, we develop an algorithm to automatically derive and compute LiRPA bounds for any computational graph, provided that the linear bounds for primitive elements (e.g., affine operations or simple activation functions) are given. Our automatic perturbation analysis algorithm is analogous to automatic differentiation (used in Tensorflow or PyTorch), where gradients are derived and computed automatically once the computational graph is defined. Moreover, our algorithm provides much more flexibility on perturbation analysis which goes beyond input perturbations within ℓ_p -balls. We summarize our main contributions below:

- For a computational graph, we provide an *automatic* procedure to derive upper and lower bounds of output nodes as linear functions of perturbed nodes, without manual derivation or implementation for the specific network architecture.
- We analyze two modes of bounds derivation for general computational graphs – forward mode and backward mode, which offer trade-off between time complexity and tightness of bounds.

- Our automatic bounds are also *differentiable*; we can take derivatives of bounds with respect to any elements in the computational graph. This allows training the bounds to provide tight and provable certificates.
- Our framework allows flexible perturbation specifications beyond ℓ_p -balls. For example, we demonstrate a *dynamic programming* approach to compute bounds under perturbation of synonym-based word substitution in a sentiment analysis task.
- We enable a number of applications that can be extremely difficult or impossible without our algorithm. We demonstrate neural network verification and certifiable training for fairly complicated neural networks, where a manual derivation and implementation can be extremely tedious even for a specific model. We also demonstrate using our algorithm as a tool to investigate a well-known hypothesis on generalization and flat optimization landscape of neural networks and train neural networks that are robust against weight perturbations.

2 Background and Related Work

Giving certified lower and upper bounds for neural networks under input perturbations is the core problem for robustness verification of neural networks. Early works formulated robustness verification for ReLU networks as satisfiability modulo theory (SMT) and integer linear programming (ILP) problems (Ehlers, 2017; Katz et al., 2017; Tjeng et al., 2019), which are hardly feasible even for a MNIST-scale small network. Wong & Kolter (2018b) proposed to relax the verification problem with linear programming and investigated its dual solution. Many other works have independently discovered similar algorithms (Dvijotham et al., 2018b; Mirman et al., 2018; Singh et al., 2018; Weng et al., 2018; Zhang et al., 2018; Singh et al., 2019b; Wang et al., 2018b) in either primal or dual space which we refer to as linear relaxation based perturbation analysis (LiRPA). Recently, Salman et al. (2019) unified these algorithms under the framework of convex relaxation. Among them, CROWN (Zhang et al., 2018) and DeepPoly (Singh et al., 2019b) achieve the tightest bound of linear relaxation and are representative algorithms of LiRPA. Several further refinements for the LiRPA bounding process were also proposed recently, including using an optimizer to choose better linear bounds (Dvijotham et al., 2018a; Lyu et al., 2019), relaxing multiple neurons (Singh et al., 2019a), but these methods typically involve much higher computational costs. The contribution of our work is to extend LiRPA to its most general form, and allow automatic derivation and computation for general network architectures. Additionally, our framework allows a general purpose perturbation analysis for any nodes in the graph and flexible perturbation specifications, not limiting to perturbations on input nodes or ℓ_p -ball perturbation specifications. This allows us to use LiRPA as a general tool beyond robustness verification.

The neural network verification problem can also be solved via many other techniques, for example, semidefinite programming (Dvijotham et al., 2019; Raghunathan et al., 2018), bounding local or global Lipschitz constant (Hein & Andriushchenko, 2017; Raghunathan et al., 2018; Zhang et al., 2019c). However, LiRPA based verification method typically scales much better than other alternatives, and is a keystone for many state-of-the-art certified defense methods. Certified adversarial defenses typically seek for a guaranteed upper bound on the error, which can be efficiently obtained using LiRPA bounds. By incorporating the bounds into the training process (which requires them to be efficient and differentiable), a network can become certifiably robust (Wong & Kolter, 2018a; Mirman et al., 2018; Wang et al., 2018a; Goyal et al., 2018; Zhang et al., 2019b).

Backpropagation (Rumelhart et al., 1986) is a classic algorithm to compute the gradients of a complex error function. Backpropagation can be applied automatically once the forward computation is defined, without manual derivation of gradients. It is essential in most deep learning frameworks, such as TensorFlow (Abadi et al., 2016) and PyTorch (Paszke et al., 2019). The backward bound propagation process in our framework is analogous to the backpropagation algorithm as our computation is also automatic once the forward propagation is defined, but we aim to automatically derive bounds for output neurons instead of computing gradients. Our algorithm is significantly more complicated than the backpropagation algorithm. On the other hand, LiRPA based bounds have been computed manually in many previous works (Wong & Kolter, 2018b; Zhang et al., 2018; Wang et al., 2018a; Maurer et al., 2018), but they mostly focus on specific types of networks (e.g., feedforward or residual networks) used for their empirical study, and do not have the flexibility to generalize to general computational graphs.

3 Algorithm

Our algorithm works on general computational graphs and computes the upper and lower bounds of nodes when input nodes or parameter nodes are perturbed within the corresponding spaces. To compute the bounds of an output node, the input nodes of all the intermediate nodes with nonlinear operations need to be bounded first, required by the linear relaxation of such intermediate nodes. We can then use a backward mode perturbation analysis to compute the bounds of the output node. However, using the same way to bound all intermediate nodes can be inefficient. Therefore, we have a more efficient forward mode perturbation analysis to compute the bounds of intermediate nodes, and then we use a backward mode perturbation analysis for the final output node only, which can produce tighter bounds than using the forward mode. A flowchart of our framework is shown in Figure 2.

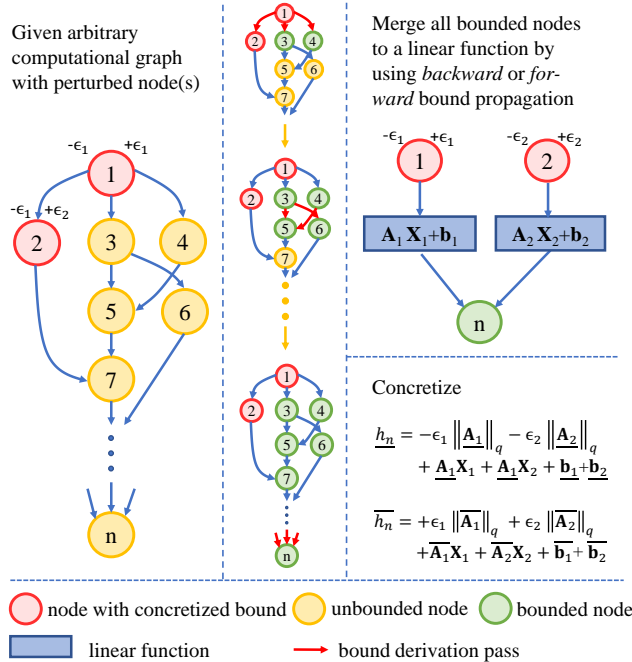


Figure 2: The flowchart of our perturbation analysis framework. Given a computational graph, we first bound all intermediate nodes, then call forward or backward bound propagation to merge intermediate nodes to a linear function w.r.t. perturbed node(s). Finally, we can concretize the bounds of output node with specific ϵ .

In the following part of this section, we will first introduce the notations, and then describe how each node supports bound propagation in perturbation analysis, and next describe the forward mode and backward mode perturbation analysis respectively. Finally, we will discuss different kinds of perturbation specifications.

3.1 Notations

Computational Graph We define a computational graph as $\mathbf{G} = (\mathbf{V}, \mathbf{E})$ which is assumed to be a Directed Acyclic Graph (DAG). $\mathbf{V} = \{v_1, v_2, \dots, v_n\}$ is a set of nodes in the graph, \mathbf{E} is a set of directed edges, and each edge $v_x \rightarrow v_y$ denotes that v_x is an input argument of v_y . We denote the computed value of v_i as vector \mathbf{h}_i . Note that although \mathbf{h}_i is a tensor in practice, we can flatten it into a vector for simplicity in describing the algorithm. Each node is either an *independent node* or a *dependent node*. The value of an independent node v_i does not rely on any other nodes and is denoted as $\mathbf{h}_i = \mathbf{x}_i$ where \mathbf{x}_i can be a vector of model input or parameters. A dependent node v_i is the output of some operation denoted as f_i taking the values of nodes $v_{u_{i,1}}, v_{u_{i,2}}, \dots, v_{u_{i,m_i}}$ as the input, where m_i is the number of input nodes and $u_{i,j} (1 \leq j \leq m_i)$ is the index of each input node:

$$\mathbf{h}_i = f_i(\mathbf{h}_{u_{i,1}}, \mathbf{h}_{u_{i,2}}, \dots, \mathbf{h}_{u_{i,m_i}}).$$

The value of an independent node v_i , i.e. \mathbf{x}_i , can be arbitrarily taken from a perturbation space \mathbb{S}_i . In particular, if \mathbf{x}_i is a fixed value and never perturbed, $\mathbb{S}_i = \{\mathbf{c}_i\}$ and $\mathbf{h}_i = \mathbf{c}_i$. We let $\mathbf{X} \in \mathbb{S}$ denote the concatenation of the values of all the independent nodes, and \mathbb{S} is the perturbation space of \mathbf{X} when each part of \mathbf{X} , i.e., each \mathbf{x}_i , is perturbed within \mathbb{S}_i respectively. Thereby, the value of each node v_i can also be regarded as a function of \mathbf{X} , i.e., $\mathbf{h}_i = h_i(\mathbf{X})$ ($\mathbf{X} \in \mathbb{S}$).

Linear Relaxation based Perturbation Analysis (LiRPA) The goal of our perturbation analysis is to compute the bounds of each $h_i(\mathbf{X})$, i.e. lower bound $\underline{\mathbf{h}}_i$ and upper bound $\overline{\mathbf{h}}_i$, when \mathbf{X} is perturbed within \mathbb{S} :

$$\underline{\mathbf{h}}_i \leq h_i(\mathbf{X}) \leq \overline{\mathbf{h}}_i \quad \forall \mathbf{X} \in \mathbb{S}, \quad (1)$$

where the comparison between two vectors is element-wise. In addition to represent the bounds with concretized values $\underline{\mathbf{h}}_i$ and $\overline{\mathbf{h}}_i$, we also compute linear bounds:

$$\underline{\mathbf{A}}^{(i)} \mathbf{X} + \underline{\mathbf{b}}^{(i)} \leq h_i(\mathbf{X}) \leq \overline{\mathbf{A}}^{(i)} \mathbf{X} + \overline{\mathbf{b}}^{(i)} \quad \forall \mathbf{X} \in \mathbb{S}, \quad (2)$$

where the bounds of $h_i(\mathbf{X})$ are represented as linear functions of \mathbf{X} , and $\underline{\mathbf{A}}^{(i)}, \underline{\mathbf{b}}^{(i)}, \overline{\mathbf{A}}^{(i)}, \overline{\mathbf{b}}^{(i)}$ are parameters. Such linear bounds can be concretized to obtain $\underline{\mathbf{h}}_i$ and $\overline{\mathbf{h}}_i$:

$$(\underline{\mathbf{h}}_i, \overline{\mathbf{h}}_i) = H(\underline{\mathbf{A}}^{(i)}, \underline{\mathbf{b}}^{(i)}, \overline{\mathbf{A}}^{(i)}, \overline{\mathbf{b}}^{(i)}), \quad (3)$$

where H is a function for bound concretization given by the corresponding perturbation specification.

During the backward mode perturbation analysis, we also represent the bounds of some node v_k with linear functions of nodes that v_k is dependent on:

$$\sum_{i=1}^n \hat{\mathbf{A}}^{(k,i)} h_i(\mathbf{X}) + \hat{\mathbf{b}}^{(k,i)} \leq h_k(\mathbf{X}) \leq \sum_{i=1}^n \overline{\hat{\mathbf{A}}}^{(k,i)} h_i(\mathbf{X}) + \overline{\hat{\mathbf{b}}}^{(k,i)} \quad \forall \mathbf{X} \in \mathbb{S}, \quad (4)$$

where $\hat{\mathbf{A}}^{(k,i)}, \hat{\mathbf{b}}^{(k,i)}, \overline{\hat{\mathbf{A}}}^{(k,i)}, \overline{\hat{\mathbf{b}}}^{(k,i)}$ are parameters and are zero matrices or vectors if v_k is not dependent on v_i . Unlike Eq. (2), bounds in Eq. (4) can be represented as linear functions of both independent and dependent nodes.

3.2 Linear Bound Propagation of Graph Nodes

To achieve perturbation analysis with the bound propagation, each node needs to support locally propagating bounds from or to its adjacent nodes. Each node v_i is associated with two functions, F_i for bound propagation in the forward mode and G_i for the backward mode, as defined below.

Forward For the forward bound propagation at node v_i , it is assumed that the linear bounds as Eq. (2) and concretized bounds as Eq. (1) of its input nodes have been computed, and F_i computes the linear bounds of v_i from the bounds of its inputs nodes:

$$(\underline{\mathbf{A}}_i, \underline{\mathbf{b}}_i, \overline{\mathbf{A}}_i, \overline{\mathbf{b}}_i) = F_i(B_{u_{i,1}}, B_{u_{i,2}}, \dots, B_{u_{i,m_i}}), \quad (5)$$

where $B_j := (\underline{\mathbf{A}}_j, \underline{\mathbf{b}}_j, \underline{\mathbf{h}}_j, \overline{\mathbf{A}}_j, \overline{\mathbf{b}}_j, \overline{\mathbf{h}}_j)$,

such that Eq. (2) holds true for v_i .

Backward In the backward mode perturbation analysis, we represent the bounds of node v_k as Eq. (4).

For a node v_i that v_k depends on, when it has non-empty $\hat{\mathbf{A}}^{(k,i)}, \overline{\hat{\mathbf{A}}}^{(k,i)}$, we aim to propagate these parameters to the input nodes of v_i , such that the lower bound of $\hat{\mathbf{A}}^{(k,i)} h_i(\mathbf{X})$ and the upper bound of $\overline{\hat{\mathbf{A}}}^{(k,i)} h_i(\mathbf{X})$ can be represented as linear functions of the input nodes of v_i , achieved by the G_i function:

$$(\hat{B}_{u_{i,1}}^{(k,i)}, \hat{B}_{u_{i,2}}^{(k,i)}, \dots, \hat{B}_{u_{i,m}}^{(k,i)}, \hat{\mathbf{b}}^{(k,i)}, \overline{\hat{\mathbf{b}}}^{(k,i)}) = G_i(\hat{\mathbf{A}}^{(k,i)}, \overline{\hat{\mathbf{A}}}^{(k,i)}), \text{ where}$$

$$\begin{aligned}
\hat{B}_{u_{i,j}}^{(k,i)} &:= (\hat{\mathbf{A}}^{(k,i,u_{i,j})}, \overline{\hat{\mathbf{A}}}^{(k,i,u_{i,j})}) \\
s.t. \quad &\sum_{j=1}^{m_i} \hat{\mathbf{A}}^{(k,i,u_{i,j})} h_{u_{i,j}}(\mathbf{X}) + \hat{\mathbf{b}}^{(k,i)} \leq \hat{\mathbf{A}}^{(k,i)} h_i(\mathbf{X}), \\
\overline{\hat{\mathbf{A}}}^{(k,i)} h_i(\mathbf{X}) &\leq \sum_{j=1}^{m_i} \overline{\hat{\mathbf{A}}}^{(k,i,u_{i,j})} h_{u_{i,j}}(\mathbf{X}) + \overline{\hat{\mathbf{b}}}^{(k,i)}, \quad \forall \mathbf{X} \in \mathbb{S}.
\end{aligned} \tag{6}$$

Such propagation is recursively applied until the bounds are finally represented as linear functions of the independent nodes while other dependent nodes are not involved, as we will describe in Sec. 3.4.

In practice, functions F and G are defined for each operation, and each node v_i reuses those functions according to its operation f_i . The bound propagation for some common operations has been derived in previous works (Zhang et al., 2019a; Ko et al., 2019; Shi et al., 2020), and we review examples of affine transformations and activation functions below, and also dot products in Appendix A.

Affine Transformation Suppose the operation of node v_i is an affine transformation with exactly one input node v_j ,

$$h_i(\mathbf{X}) = \tilde{\mathbf{W}}_i h_j(\mathbf{X}) + \tilde{\mathbf{b}}, \tag{7}$$

where $\tilde{\mathbf{W}}$ is the weight matrix and $\tilde{\mathbf{b}}$ is the bias vector. For the forward bound propagation, the upper bound of $h_i(\mathbf{X})$ can be computed by multiplying positive weights with the upper bound of $h_j(\mathbf{X})$ and negative weights with the lower bound of $h_j(\mathbf{X})$, and the lower bound can also be computed vice versa. Thereby, F_i can be defined as:

$$\begin{aligned}
\underline{\mathbf{A}}^{(i)} &= \tilde{\mathbf{W}}_+ \underline{\mathbf{A}}^{(j)} + \tilde{\mathbf{W}}_- \overline{\mathbf{A}}^{(j)}, \quad \underline{\mathbf{b}}^{(i)} = \tilde{\mathbf{W}}_+ \underline{\mathbf{b}}^{(j)} + \tilde{\mathbf{W}}_- \overline{\mathbf{b}}^{(j)} + \tilde{\mathbf{b}}, \\
\overline{\mathbf{A}}^{(i)} &= \tilde{\mathbf{W}}_+ \overline{\mathbf{A}}^{(j)} + \tilde{\mathbf{W}}_- \underline{\mathbf{A}}^{(j)}, \quad \overline{\mathbf{b}}^{(i)} = \tilde{\mathbf{W}}_+ \overline{\mathbf{b}}^{(j)} + \tilde{\mathbf{W}}_- \underline{\mathbf{b}}^{(j)} + \tilde{\mathbf{b}},
\end{aligned}$$

where $\tilde{\mathbf{W}}_+$ stands for retaining positive elements in $\tilde{\mathbf{W}}$ and vice versa. And for G_i , we substitute $h_i(\mathbf{X})$ in $\hat{\mathbf{A}}^{(k,i)} h_i(\mathbf{X})$ and $\overline{\hat{\mathbf{A}}}^{(k,i)} h_i(\mathbf{X})$ with Eq. (7), and thus we have:

$$\begin{aligned}
\hat{\mathbf{A}}^{(k,i,j)} &= \hat{\mathbf{A}}^{(k,i)} \cdot \tilde{\mathbf{W}}, & \overline{\hat{\mathbf{A}}}^{(k,i,j)} &= \overline{\hat{\mathbf{A}}}^{(k,i)} \cdot \tilde{\mathbf{W}}, \\
\hat{\mathbf{b}}^{(k,i)} &= \hat{\mathbf{A}}^{(k,i)} \cdot \tilde{\mathbf{b}}, & \overline{\hat{\mathbf{b}}}^{(k,i)} &= \overline{\hat{\mathbf{A}}}^{(k,i)} \cdot \tilde{\mathbf{b}}.
\end{aligned}$$

Activation Functions Suppose the operation of node v_i is an activation function and has exactly one input node v_j ,

$$h_i(\mathbf{X}) = \sigma(h_j(\mathbf{X})),$$

where $\sigma(\cdot)$ denotes some activation function. With the concretized bounds of $h_j(\mathbf{X})$, i.e. $\underline{\mathbf{h}}_j$ and $\overline{\mathbf{h}}_j$, $\sigma(h_j(\mathbf{X}))$ can be relaxed with linear bounds:

$$\underline{\mathbf{D}} h_j(\mathbf{X}) + \underline{\mathbf{c}} \leq \sigma(h_j(\mathbf{X})) \leq \overline{\mathbf{D}} h_j(\mathbf{X}) + \overline{\mathbf{c}}, \quad \forall \underline{\mathbf{h}}_j \leq h_j(\mathbf{X}) \leq \overline{\mathbf{h}}_j,$$

where diagonal matrices $\underline{\mathbf{D}}, \overline{\mathbf{D}}$ and vectors $\underline{\mathbf{c}}, \overline{\mathbf{c}}$ are the parameters of the linear relaxation derived for the specific activation function as shown in Appendix A. Then for F_i :

$$\begin{aligned}
\underline{\mathbf{A}}^{(i)} &= \underline{\mathbf{D}}_+ \underline{\mathbf{A}}^{(j)} + \underline{\mathbf{D}}_- \overline{\mathbf{A}}^{(j)}, \quad \underline{\mathbf{b}}^{(i)} = \underline{\mathbf{D}}_+ \underline{\mathbf{b}}^{(j)} + \underline{\mathbf{D}}_- \overline{\mathbf{b}}^{(j)} + \underline{\mathbf{c}}_i, \\
\overline{\mathbf{A}}^{(i)} &= \overline{\mathbf{D}}_+ \overline{\mathbf{A}}^{(j)} + \overline{\mathbf{D}}_- \underline{\mathbf{A}}^{(j)}, \quad \overline{\mathbf{b}}^{(i)} = \overline{\mathbf{D}}_+ \overline{\mathbf{b}}^{(j)} + \overline{\mathbf{D}}_- \underline{\mathbf{b}}^{(j)} + \overline{\mathbf{c}}_i,
\end{aligned}$$

where $\underline{\mathbf{D}}_+$ and $\overline{\mathbf{D}}_+$ stands for only retaining positive elements in $\underline{\mathbf{D}}$ and $\overline{\mathbf{D}}$ respectively, and vice versa for $\underline{\mathbf{D}}_-$ and $\overline{\mathbf{D}}_-$. And for G_i :

$$\begin{aligned}\hat{\underline{\mathbf{A}}}^{(k,i,j)} &= \hat{\underline{\mathbf{A}}}_+^{(k,i)} \cdot \underline{\mathbf{D}} + \hat{\underline{\mathbf{A}}}_-^{(k,i)} \cdot \overline{\mathbf{D}}, \\ \overline{\hat{\underline{\mathbf{A}}}}^{(k,i,j)} &= \overline{\hat{\underline{\mathbf{A}}}}_+^{(k,i)} \cdot \overline{\mathbf{D}} + \overline{\hat{\underline{\mathbf{A}}}}_-^{(k,i)} \cdot \underline{\mathbf{D}}, \\ \hat{\underline{\mathbf{b}}}^{(k,i,j)} &= \hat{\underline{\mathbf{A}}}_+^{(k,i)} \cdot \underline{\mathbf{c}} + \hat{\underline{\mathbf{A}}}_-^{(k,i)} \cdot \overline{\mathbf{c}}, \\ \overline{\hat{\underline{\mathbf{b}}}}^{(k,i,j)} &= \overline{\hat{\underline{\mathbf{A}}}}_+^{(k,i)} \cdot \overline{\mathbf{c}} + \overline{\hat{\underline{\mathbf{A}}}}_-^{(k,i)} \cdot \underline{\mathbf{c}}.\end{aligned}$$

We provide a detailed explanation in Appendix A.

3.3 General Forward Mode Perturbation Analysis

Algorithm 1 Forward Mode Bound Propagation

```

function BoundForward( $v_i$ )
  for  $1 \leq j \leq m$  do
    if bounds of  $v_{u_{i,j}}$  unavailable then
      BoundForward( $v_{u_{i,j}}$ )
     $(\underline{\mathbf{A}}^{(i)}, \underline{\mathbf{b}}^{(i)}, \overline{\mathbf{A}}^{(i)}, \overline{\mathbf{b}}^{(i)}) = F_i(B_{u_{i,1}}, \dots, B_{u_{i,m_i}})$  (Eq. (5))
     $(\underline{\mathbf{h}}_i, \overline{\mathbf{h}}_i) = H(\underline{\mathbf{A}}^{(i)}, \underline{\mathbf{b}}^{(i)}, \overline{\mathbf{A}}^{(i)}, \overline{\mathbf{b}}^{(i)})$  (Eq. (3))

```

The linear bounds of independent node v_i is $\mathbf{x}_i \leq h_i(\mathbf{X}) \leq \mathbf{x}_i$ since $h_i(\mathbf{X}) = \mathbf{x}_i$, from which the parameters in Eq. (2) can be easily obtained, and they can be concretized with function H . For any dependent node v_i , we can obtain its bounds by recursively applying Eq. (5) and Eq. (3), i.e. the bounds of any node can be propagated from nodes it depends on in a forward manner. We formulate the algorithm for dependent nodes with Algorithm 1. In this algorithm, to compute the bounds of v_i , we first check its input nodes. For any input node $v_{u_{i,j}}$, if its bounds are not available yet, we first call the algorithm recursively to compute the bounds of $v_{u_{i,j}}$. After the bounds of all the input nodes are available, we use the F_i function to obtain the the linear bounds of v_i , and then concretize the linear bounds with the H function.

3.4 General Backward Mode Perturbation Analysis

Theorem 1. For a dependent node v_k , its bounds can be represented with linear functions of nodes that v_k depends on, as shown in Eq. (4). The inequality holds true initially with:

$$\hat{\underline{\mathbf{A}}}^{(k,k)} = \overline{\hat{\underline{\mathbf{A}}}}^{(k,k)} = \mathbf{I}, \quad \hat{\underline{\mathbf{A}}}^{(k,i)} = \overline{\hat{\underline{\mathbf{A}}}}^{(k,i)} = \mathbf{0} \quad (\forall i \neq k), \quad (8)$$

$$\hat{\underline{\mathbf{b}}}^{(k)} = \overline{\hat{\underline{\mathbf{b}}}}^{(k)} = \mathbf{0}. \quad (9)$$

By recursively applying Eq. (6), the parameters can be propagated such that Eq. (4) still holds true while $\hat{\underline{\mathbf{A}}}^{(k,i)}$ and $\overline{\hat{\underline{\mathbf{A}}}}^{(k,i)}$ are non-zero only if v_i is an independent node.

Linear bounds of a dependent node v_k can also be computed via a backward process, as summarized in Theorem 1. The proof is provided in Appendix B. Based on this, we design a general backward mode perturbation analysis algorithm. We first define an auxiliary algorithm, a ‘‘GetDegree’’ function, detailed in Appendix D, which uses a BFS to compute degree d_i for each node v_i , which denotes the number of output nodes of v_i that v_k is dependent on. We next use another BFS for propagating the linear bounds, which starts from v_k with the parameters set as Eq. (8) and Eq. (9). For each node v_i picked from the head of the queue, we call G_i function to propagate the terms regarding $h_i(\mathbf{X})$ and bound them with linear functions of the input nodes of v_i as Eq. (6). We then accumulate the bound parameters of terms regarding each $h_{u_{i,j}}(\mathbf{X})$,

the following problem:

$$\underline{\mathbf{h}}_i = \min_{\mathbf{X} \in \mathbb{S}} \underline{\mathbf{A}}^{(i)} \mathbf{X} + \underline{\mathbf{b}}^{(i)}, \quad \bar{\mathbf{h}}_i = \max_{\mathbf{X} \in \mathbb{S}} \bar{\mathbf{A}}^{(i)} \mathbf{X} + \bar{\mathbf{b}}^{(i)}.$$

We show two examples of perturbation specifications in this section: ℓ_p -ball perturbations and synonym-based word substitution.

ℓ_p -ball Perturbations In this setting, assuming that $\mathbf{X} = \mathbf{X}_0$ if \mathbf{X} is clean and not perturbed, the perturbation space is defined by $\mathbb{S} = \{\mathbf{X} \mid \|\mathbf{X} - \mathbf{X}_0\|_p \leq \epsilon\}$, which means that \mathbf{X} is perturbed within an ℓ_p -ball centered at \mathbf{X}_0 with a radius of ϵ . The linear bounds can be concretized as follows (Zhang et al., 2018):

$$\begin{aligned} \underline{\mathbf{h}}_i &= -\epsilon \|\underline{\mathbf{A}}^{(i)}\|_q + \underline{\mathbf{A}}^{(i)} \mathbf{X}_0 + \underline{\mathbf{b}}^{(i)}, \\ \bar{\mathbf{h}}_i &= \epsilon \|\bar{\mathbf{A}}^{(i)}\|_q + \bar{\mathbf{A}}^{(i)} \mathbf{X}_0 + \bar{\mathbf{b}}^{(i)}, \end{aligned}$$

where $1/p + 1/q = 1$ ($p \geq 1$), and $\|\cdot\|_q$ denotes taking ℓ_q -norm for each row in the matrix and the result makes up a vector.

Synonym-based Word Substitution Beyond ℓ_p -ball specifications, our algorithm also supports perturbation spaces consisting of discrete points, which are more practical for applications such as NLP tasks. In this setting, we assume that the clean input to the model is a sequence of words w_1, w_2, \dots, w_l mapped to embeddings $e(w_1), e(w_2), \dots, e(w_l)$. Following a common adversarial perturbation setting in NLP (Huang et al., 2019; Jia et al., 2019), we allow at most δ words to be replaced and each word w_i can be replaced by words within its pre-defined substitution set $\mathbb{S}(w_i)$ constructed from its synonyms and further validated with a language model. We denote each actual input word as $\hat{w}_i \in \{w_i\} \cup \mathbb{S}(w_i)$ when the perturbation is considered, and we include details about constructing the substitution word sets in Appendix E. We show that the linear bounds of node v_k can be concretized with dynamic programming.

Theorem 2. *The lower bound of*

$$\underline{\mathbf{b}}^{(k)} + \sum_{t=1}^i \underline{\mathbf{A}}_{:, \#t}^{(k)} e(\hat{w}_t), \quad (10)$$

when j words among $\hat{w}_1, \dots, \hat{w}_i$ have been replaced, denoted as $\underline{\mathbf{g}}_{i,j}$, can be computed by:

$$\underline{\mathbf{g}}_{i,j} = \min(\underline{\mathbf{g}}_{i-1,j} + \underline{\mathbf{A}}_{:, \#i}^{(k)} e(w_i), \underline{\mathbf{g}}_{i-1,j-1} + \min_{w' \in \mathbb{S}(w_i)} \{\underline{\mathbf{A}}_{:, \#i}^{(k)} e(w')\}) \quad (i, j > 0),$$

and $\underline{\mathbf{g}}_{i,0} = \underline{\mathbf{b}}^{(k)} + \sum_{t=1}^i \underline{\mathbf{A}}_{:, \#t}^{(k)} e(w_t)$, where $\underline{\mathbf{A}}_{:, \#i}^{(k)} = \underline{\mathbf{A}}_{:, (\tilde{d} \times (i-1) + 1): (\tilde{d} \times i)}^{(k)}$ and \tilde{d} denotes the dimension of each embedding $e(w_i)$ and $e(\hat{w}_i)$, and thereby $\underline{\mathbf{A}}_{:, \#i}^{(k)}$ corresponds to the coefficients of $e(\hat{w}_i)$ in the linear bounds.

As illustrated in Theorem 2, $\underline{\mathbf{g}}_{i,j}$ is computed by dynamic programming. For $j=0$, $\hat{w}_1, \hat{w}_2, \dots, \hat{w}_i$ must have not been replaced and thus $\hat{w}_t = w_t$ ($1 \leq t \leq i$) holds true. For $i, j > 0$, the dynamic programming considers whether \hat{w}_i has been replaced. If \hat{w}_i has not been replaced, the term regarding $t=i$ in Eq. (10) is exactly $\underline{\mathbf{A}}_{:, \#i}^{(k)} e(w_i)$, and j words have been replaced among the first $i-1$ words. In this case, we have $\underline{\mathbf{g}}_{i-1,j} + \underline{\mathbf{A}}_{:, \#i}^{(k)} e(w_i)$ for Eq. (10). Otherwise, the lower bound of $\underline{\mathbf{A}}_{:, \#i}^{(k)} e(\hat{w}_i)$ needs to be taken from the minimum value of $\underline{\mathbf{A}}_{:, \#i}^{(k)} e(w')$ when w' can be any substitution word of w_i , i.e. $w' \in \mathbb{S}(w_i)$, and $\underline{\mathbf{g}}_{i,j}$ is transferred from $\underline{\mathbf{g}}_{i-1,j-1}$ where $j-1$ words are replaced in the first $i-1$ words. The dynamic programming takes the minimum value from these two cases as $\underline{\mathbf{g}}_{i,j}$. Finally, $\underline{\mathbf{h}}_k = \min_{0 \leq j \leq \delta} \underline{\mathbf{g}}_{i,j}$ is the result of the concretization by enumerating the number of replaced words $0 \leq j \leq \delta$. The upper bounds can also be computed in a similar way simply by changing from taking the minimum to taking the maximum in the above derivation.

4 Experiments

We implement our algorithm using PyTorch (Paszke et al., 2019). Given any neural network model implemented as a PyTorch module, we first extract its computational graph from the trace of the model. The our algorithm

traverses this graph and automatically creates the necessary computation for perturbation analysis. Our implementation enables automatic perturbation analysis for any computational graph defined in PyTorch as long as elementary operations involved are supported. Therefore, it can be used to verify or conduct certified training for a wide range of neural models. We demonstrate several interesting applications of our algorithm below.

4.1 Robustness Verification for Sentiment Classification

We first use our algorithm to verify the robustness of a Transformer model for sentiment classification under synonym-based word substitution. This demonstrates our flexibility in handling complex models such as Transformer, and showcases our novel discrete perturbation specification for LiRPA described in Sec. 3.5.

We use the SST-2 dataset (Socher et al., 2013) consisting of 6,920/872/1,821 examples in the training/development/test set. Each example is a sentence labeled with a sentiment polarity (2 classes), and each phrase on the parse tree of the sentence is also labeled with a sentiment polarity and can be used for training in addition to the whole sentence. We verify a one-layer Transformer (Vaswani et al., 2017) trained from scratch, and we report the details of this model in Appendix F. For the perturbation specification of synonym-based word substitution, we use $1 \leq \delta \leq 6$ (up to 6 word substitutions). In this model, the logits layer is the final output node that we aim to bound. We evaluate the *verified accuracy* with the worst-case logits under perturbation, i.e., we take the lower bound for the correct label and take the upper bound for the incorrect one (which was done similarly in (Wong & Kolter, 2018b; Zhang et al., 2019a)). We use four different configurations for verification: an Interval Bound Propagation (IBP) baseline (Huang et al., 2019) which only has concretized bounds and no linear terms, and we review it in Appendix G; a “forward” configuration where we fully use the forward mode perturbation analysis for all nodes; and “IBP→backward” and “Forward→backward” configurations, where we use IBP or the forward mode for bounding all intermediate nodes while using the backward mode perturbation analysis for the final output node. In addition, we also include results computed by an *oracle* algorithm for reference, which enumerates *all* the possible perturbed sequences, but it has an exponential complexity and is thus too inefficient to be further used for certified training that we will conduct.

Standard Accuracy (%)	Configuration	Verified Accuracy (%)					
		$\delta = 1$	$\delta = 2$	$\delta = 3$	$\delta = 4$	$\delta = 5$	$\delta = 6$
82.5	IBP	4.6	1.8	1.0	0.9	0.8	0.8
	IBP→backward	25.6	7.7	3.8	2.5	2.5	2.5
	Forward	63.3	51.0	43.5	39.3	38.1	37.1
	Forward→backward	65.5	54.4	47.2	43.4	41.6	40.8
	Oracle	66.0	55.1	47.9	44.1	42.0	41.2

Table 1: Results of verifying a normally trained Transformer, where δ is the budget for word substitution. “Oracle” verified accuracy is based on brute-force enumeration, and for each verification configuration, verified accuracy closer to Oracle is better.

Our results are shown in Table 1. The pure IBP configuration produces very loose bounds and thereby very small verified accuracies. In contrast, other configurations with LiRPA produce higher verified accuracies. Using a backward mode perturbation analysis on the final output layer produces tighter bounds than using the forward mode or IBP for all nodes (“forward→backward” v.s. “forward” and “IBP→backward” v.s. “IBP”), demonstrating the effectiveness of the backward mode perturbation analysis. The results given by the oracle algorithm are the upper bounds that any verification algorithm can achieve, while the results by “forward→backward” are already very close to those by oracle. Moreover, the accuracies by all the four configurations are smaller than those by the oracle algorithm with the corresponding δ , which is consistent with the goal that our perturbation analysis computes worst-case logits and gives the lower bound of robustness. The results demonstrate that automatic LiRPA bounds computed by our algorithm can more effectively and tightly verify the robustness of the Transformer model. compared to the baseline using IBP only.

4.2 Certified Robust Training

Since the bounds computed by our algorithm are differentiable, we can then leverage them to conduct certifiable robust training, a.k.a., certified defense. Note that without our framework, previous works are only able to implement very simple algorithms such as IBP for certified defense on NLP models (Jia et al., 2019;

Huang et al., 2019). We will show that training on LiRPA bounds that are much tighter than IBP bounds can lead to significantly improved robust models. The objective of robust training is:

$$\min_{\theta} \mathbb{E}_{\mathbf{X} \in \mathbb{D}} [(1 - \kappa)\mathcal{L}(h(\mathbf{X}, \epsilon = 0); y; \theta) + \kappa\mathcal{L}(\bar{h}(\mathbf{X}, \epsilon); y; \theta)]$$

where the first term in the expectation is a normal cross entropy loss, and the second term is a robust loss term, i.e., worst-case cross entropy loss from our perturbation analysis, and $0 \leq \kappa \leq 1$ is a scalar hyperparameter to balance the two loss terms. ϵ is a hyperparameter to artificially shrink the perturbation bounds of input nodes, which is linearly increased from 0 to 1 during the warmup stage (Jia et al., 2019) (sometimes this procedure is referred to as “ ϵ scheduling”). We train a Transformer and an LSTM as the sentiment classifier. We do not verify a normally trained LSTM in Table 1 because its robust accuracy is almost 0 by all configurations, due to the long computation paths (Jia et al., 2019). We train the models with $\delta = 3$ but test them on all $1 \leq \delta \leq 6$ following Huang et al. (2019). For our training method, we use the “IBP→backward” configuration for efficiency. We report more details about our robust training in Appendix F.

Model	Method	Standard Accuracy (%)	Verified Accuracy (%)					
			$\delta = 1$	$\delta = 2$	$\delta = 3$	$\delta = 4$	$\delta = 5$	$\delta = 6$
LSTM	IBP	73.9	66.3	64.5	63.4	60.6	55.4	48.2
	Ours	79.3	75.2	73.0	71.7	70.5	69.0	66.4
Transformer	IBP	82.1	81.1	80.0	78.8	77.2	75.5	74.0
	Ours	82.5	80.7	80.2	79.8	79.4	78.3	75.7

Table 2: Results of certified robust training for LSTM and Transformer using IBP and our algorithm respectively, where “standard accuracy” denotes the accuracy evaluated without perturbation, “verified accuracy” denotes the accuracy when the input can be perturbed within the defined space, δ denotes the test budget and all the models are trained with $\delta = 3$.

Table 2 shows our results. The LSTM model trained with our algorithm using “IBP→backward” configuration achieves much higher verified accuracy numbers compared with those by IBP. Transformer trained by our algorithm using “IBP→backward” configuration also outperforms that by IBP for $2 \leq \delta \leq 6$. This shows the advantage of using a tight bound given by backward mode perturbation analysis during training. Transformer by IBP performs slightly better than that by our algorithm for $\delta = 1$, mainly because the perturbation space is too small in this setting and the models are already relatively robust, and thus our tighter bounds have limited advantages. Compared to results on naturally trained Transformer in Table 1, the Transformer with robust training achieves much higher verified accuracy; additionally, LSTM also achieves high verified accuracy after robust training using LiRPA bounds (a naturally trained LSTM has close to 0% verified accuracy on this task). The results demonstrate that our algorithm can effectively train certifiably robust models and outperform the IBP baseline when δ is not too small.

The use of an automatic framework for LiPRA is important for this task and allows us to achieve state-of-the-art results; using the same SST dataset, verified accuracy reported by (Huang et al., 2019) are below 50% for $\delta = 6$. Previous works (Jia et al., 2019; Huang et al., 2019) can only utilize simple models (CNN or LSTM) and simple bound propagation method (IBP) for certifiable training due to bound derivation and implementation difficulty. Our algorithm allows us to train on complex models like Transformer and use the much tighter but more complicated backward mode perturbation analysis method.

4.3 Training Neural Networks with Guaranteed Flatness

Background. Recently, some researchers (He et al., 2019; Jastrzebski et al., 2018; Goyal et al., 2017; Hoffer et al., 2017) have hypothesized that DNNs optimized with stochastic gradient descent (SGD) can find wide and flat local minima which may be associated with good generalization performance. Unlike most previous works on verification or certified defense where only input perturbation is allowed, our framework naturally extends perturbation analysis on network parameters $\theta := [\mathbf{w}_1, \mathbf{w}_2, \dots, \mathbf{w}_K]$ (weight vectors of all K layers concatenated) as each weight \mathbf{w}_i are also inputs of the computational graph (we ignore bias for simplicity). Based on this advantage, we can guarantee the local “flatness” around a certain point θ_0 for some loss \mathcal{L} :

$$\mathcal{L}(\theta_0) - C_L \leq \mathcal{L}(\theta_0 + \Delta\theta) \leq \mathcal{L}(\theta_0) + C_U, \text{ for all } \|\Delta\theta\|_2 \leq \epsilon \quad (11)$$

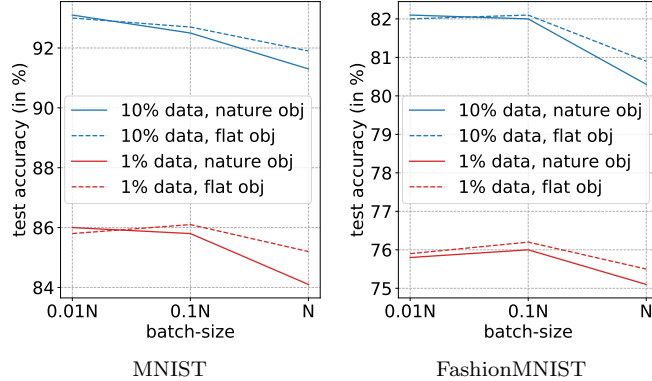


Figure 4: Test accuracy naturally trained models and models trained using the LiRPA based “flat” objective (12) on MNIST and FashionMNIST with different combination of data size and batch size. Using objective (12) noticeably improves generalization especially when less data and bigger batch sizes are used.

Where C_L and C_U are two small positive numbers. This is a “zeroth order” flatness criterion, where we guarantee that the loss value does not change too much for a small region around θ_0 , and we do not have further assumptions on gradients or Hessian of the loss. For convenience, we define a set $\mathbb{S}(\mathbf{w}) = \{\mathbf{w} : \|\mathbf{w} - \mathbf{w}_i\|_2 \leq \epsilon_i\}$, $\epsilon = [\epsilon_1, \dots, \epsilon_K]$ to represent perturbation budget for each layer’s weight parameter.

When θ_0 is a good solution, $\mathcal{L}(\theta_0)$ is close to 0 so we can simply set the left hand side of (11) to 0, and upper bound $\mathcal{L}(\theta_0 + \Delta\theta)$. Using our framework, we can train a classifier that guarantees flatness of local optimization landscape, by upper bounding the loss under weight perturbations:

$$\max_{\mathbf{w} \in \mathbb{S}} \mathcal{L}(\theta) = \max_{\mathbf{w} \in \mathbb{S}} \mathbb{E}_{\{\mathbf{x}, y\} \in \mathbb{D}} L(h(\mathbf{x}, \theta), y) \leq \mathbb{E}_{\{\mathbf{x}, y\} \in \mathbb{D}} L(-\underline{h}_I(\mathbf{x}, \theta, \epsilon), y) \quad (12)$$

where $\underline{h}_I(\mathbf{x}, \theta, \epsilon)$ denotes the lower bound of margins between the logit of y and all other classes with perturbation on each layer’s weight, defined similarly as in (Zhang et al., 2019a). The last inequality is from Theorem 2 in (Wong & Kolter, 2018b) and we assume L is cross-entropy loss with softmax. Using our algorithm we can obtain LiRPA bounds in the form of

$$\underline{h}_I = \min_{\mathbf{w} \in \mathbb{S}} \sum_i \underline{\mathbf{A}}^{(i)} \mathbf{w}_i + \underline{\mathbf{A}}^{(x)} \mathbf{x} + \underline{\mathbf{b}}^{(I)},$$

here we treat weights \mathbf{w} as the inputs under perturbation in the computational graph, and keep data examples \mathbf{x} intact. After concretization we get

$$\underline{h}_I = \sum_i (-\epsilon_i \|\underline{\mathbf{A}}^{(i)}\|_2 + \underline{\mathbf{A}}^{(i)} \mathbf{w}_i) + \underline{\mathbf{A}}^{(x)} \mathbf{x} + \underline{\mathbf{b}}^{(I)}. \quad (13)$$

Finally, substituting \underline{h}_I in Eq. (12) with Eq. (13), we can minimize a cross entropy loss $\mathbb{E}_{\{\mathbf{x}, y\} \in \mathbb{D}} L(-\underline{h}_I(\mathbf{x}, \theta, \epsilon), y)$; when this loss is minimized, an upper of $\mathcal{L}(\theta)$ for any $\mathbf{w} \in \mathbb{S}$ is minimized. In other words, the landscape near this local minimum is “flat” as defined in (11). Now we provide details of our experiments.

Setup. Based on the training loss (12), we build a three-layer MLP model with [64, 64, 10] neurons in each layer and conduct experiments by using only 10% and 1% of the training data in MNIST and FashionMNIST, and we then test on full test set to aggressively evaluate the generalization performance. We also aggressively set the batch size to $\{0.01N, 0.1N, N\}$ as in (Jastrzebski et al., 2018) where N is the size of training dataset. We use the backward mode perturbation analysis (Algorithm 2) for this experiment. No existing works attempted to train a LiRPA based bounds under weight perturbations.

Generalization Performance. The test accuracies of models trained with regular cross entropy and the “flat” objective (12) are shown in Figure 4. When batch size is increased or less data is used, test accuracy generally decreases due to overfitting, which is consistent with Keskar et al. (2016). For models trained

with the flat objective, accuracy tends to be better, especially when a very large batch size is used. These observations provide some evidence for the hypothesis that a flat local minimum generalizes better, however we cannot exclude the possibility that the improvements on accuracy come from side effects of the objective (11). The focus of this paper is to demonstrate potential applications of our algorithm rather than proving this hypothesis.

Certified Flatness. Using bounds obtained from LiRPA, we can obtain a certified upper bound on training loss. We define the flatness based on certified training cross entropy loss at a point $\theta^* = [\mathbf{w}_1^*, \mathbf{w}_2^*, \dots, \mathbf{w}_K^*]$ as:

$$\mathcal{F} = \mathcal{L}(-\underline{h}_T(\mathbf{x}, \theta^*, \epsilon); y) - \mathcal{L}(h(\mathbf{x}, \theta^*); y) \geq \max_{\mathbf{w} \in \mathcal{S}} \mathcal{L}(\theta) - \mathcal{L}(\theta^*)$$

where $\underline{h}_T(\mathbf{x}, \theta^*, \epsilon)$ is defined similarly as in (12). A small \mathcal{F} guarantees that \mathcal{L} does not change wildly around θ^* . Note that since the weight of each layer can be in quite different scales, we use a normalized $\bar{\epsilon} = 0.01$ and set $\epsilon_i = \|\mathbf{w}_i\|_2 \bar{\epsilon}$. This also allows us to make fair comparisons between models with weights in different scales. The flatness \mathcal{F} of the models we obtained are shown in Table 3.

	MNIST					
	nature training			"flat" objective		
	0.01N	0.1N	N	0.01N	0.1N	N
10%	2.50	3.24	4.48	0.86	1.04	1.77
1%	2.42	2.94	4.87	0.82	0.98	1.40
	FashionMNIST					
10%	7.48	7.79	9.56	2.39	1.80	1.92
1%	7.44	6.39	9.37	2.31	1.77	1.95

Table 3: The flatness \mathcal{F} of naturally trained models and models trained using the "flat" objective (23) with different dataset sizes (10%, 1%) and batch sizes (0.01N, 0.1N, N). A small \mathcal{F} guarantees that \mathcal{L} does not change wildly around θ^* (model parameters found by SGD). The flat objective provably reduces the range of objective around θ^* .

Robustness under Weight Perturbations. Our training objective (12) essentially produces a robust model under weight perturbations. Usually, adversarial attacks (Xu et al., 2019a,b; Chen et al., 2017) are conducted on input examples rather than weights; but here we consider an unusual threat model that model weights are under adversarial perturbation. We adapt a projected gradient descent (PGD) based attack to model weights, which can be seen as an empirical evaluation for model flatness. We select the model trained with 10% data and a batch size of 0.01N on both MNIST and FashionMNIST, and then we maximize the cross entropy loss over the whole testing data using a 10-step PGD. In each step, we clip the ℓ_2 -norm of gradients by the $\bar{\epsilon}/10$ (note that this is the normalized $\bar{\epsilon}$ and the effective $\bar{\epsilon}_i = \|\mathbf{w}_i\|_2 \bar{\epsilon}$). The "attack" results of the two models under different $\bar{\epsilon}$ are presented in Figure 5. It demonstrates that even on wilder choices of $\bar{\epsilon}$, our robustly trained models always yield better test accuracy and more stable loss than naturally trained models.

	MNIST		FashionMNIST	
	nature	robust	nature	robust
No quantization	94.95%	93.15%	83.71%	81.34%
2-bit (4 values)	88.74%	89.80%	71.27%	77.35%
Ternary	79.20%	86.95%	69.31%	76.02%

Table 4: Quantization results on MNIST and FashionMNIST. Models trained using the LiRPA based objective (12) demonstrate distinctly better performance after aggressive weight quantization.

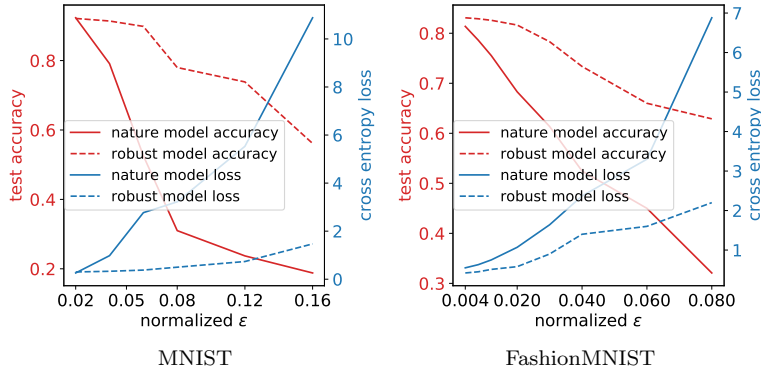


Figure 5: Test accuracy and loss on MNIST and FashionMNIST dataset under ℓ_2 weight perturbation. The accuracy of a naturally trained model can drop significantly under small perturbations on weights, and our robustly trained model using objective (12) greatly improves accuracy under weight perturbations.

Robust Weights Training Meets Quantization. By imposing ℓ_∞ perturbation on weights, namely, $\mathbb{S}(\mathbf{w}) = \{\mathbf{w}' : \|\mathbf{w}' - \mathbf{w}\|_\infty \leq \epsilon_i\}$, training using the LiRPA based objective (12) can produce a model that is insensitive to perturbation of individual weight values, which can be helpful for keeping model accuracy after aggressive quantization. Thus, we conduct weight quantization experiments on MNIST and FashionMNIST using robustly trained models against ℓ_∞ weight perturbations. We follow Han et al. (2015) by using K-means to cluster weights and replace all weights in a neural network to 3 (Ternary) or 4 (2-bit) unique values. The test accuracy on naturally trained and our robust models are shown in Table 4. The results show that by leveraging the LiRPA based training objective, when quantizing a well-trained model to 2-bit or even ternary values, our robust models achieve distinctly better test accuracy compared with naturally trained models. It demonstrates that our framework can improve the stability against weight distortion and benefit weight quantization. We provide additional weight perturbation experiments in Appendix H.

5 Conclusions

We built a novel automatic perturbation analysis framework for general neural network structures with general perturbation specifications. Our framework can also be used for certified training. We not only demonstrated a few applications and effectiveness of our framework but also provided huge potential for future LiRPA works to avoid “reinventing the wheel” on different network structures or perturbation specifications.

Acknowledgement

This work was performed under the auspices of the U.S. Department of Energy by Lawrence Livermore National Laboratory under Contract DE-AC52-07NA27344.

References

- Abadi, M., Agarwal, A., Barham, P., Brevdo, E., Chen, Z., Citro, C., Corrado, G. S., Davis, A., Dean, J., Devin, M., Ghemawat, S., Goodfellow, I., Harp, A., Irving, G., Isard, M., Jia, Y., Jozefowicz, R., Kaiser, L., Kudlur, M., Levenberg, J., Mane, D., Monga, R., Moore, S., Murray, D., Olah, C., Schuster, M., Shlens, J., Steiner, B., Sutskever, I., Talwar, K., Tucker, P., Vanhoucke, V., Vasudevan, V., Viegas, F., Vinyals, O., Warden, P., Wattenberg, M., Wicke, M., Yu, Y., and Zheng, X. Tensorflow: Large-scale machine learning on heterogeneous distributed systems, 2016.
- Alzantot, M., Sharma, Y., Elgohary, A., Ho, B.-J., Srivastava, M., and Chang, K.-W. Generating natural language adversarial examples. In *EMNLP*, pp. 2890–2896, 2018.

- Balunovic, M., Baader, M., Singh, G., Gehr, T., and Vechev, M. Certifying geometric robustness of neural networks. In *Advances in Neural Information Processing Systems*, pp. 15287–15297, 2019.
- Chen, P.-Y., Zhang, H., Sharma, Y., Yi, J., and Hsieh, C.-J. Zoo: Zeroth order optimization based black-box attacks to deep neural networks without training substitute models. In *Proceedings of the 10th ACM Workshop on Artificial Intelligence and Security*, pp. 15–26. ACM, 2017.
- Dvijotham, K., Gowal, S., Stanforth, R., Arandjelovic, R., O’Donoghue, B., Uesato, J., and Kohli, P. Training verified learners with learned verifiers. *arXiv preprint arXiv:1805.10265*, 2018a.
- Dvijotham, K., Stanforth, R., Gowal, S., Mann, T., and Kohli, P. A dual approach to scalable verification of deep networks. *UAI*, 2018b.
- Dvijotham, K. D., Stanforth, R., Gowal, S., Qin, C., De, S., and Kohli, P. Efficient neural network verification with exactness characterization. *UAI*, 2019.
- Ehlers, R. Formal verification of piece-wise linear feed-forward neural networks. In *International Symposium on Automated Technology for Verification and Analysis*, pp. 269–286. Springer, 2017.
- Gowal, S., Dvijotham, K., Stanforth, R., Bunel, R., Qin, C., Uesato, J., Mann, T., and Kohli, P. On the effectiveness of interval bound propagation for training verifiably robust models. *arXiv preprint arXiv:1810.12715*, 2018.
- Goyal, P., Dollár, P., Girshick, R., Noordhuis, P., Wesolowski, L., Kyrola, A., Tulloch, A., Jia, Y., and He, K. Accurate, large minibatch sgd: Training imagenet in 1 hour. *arXiv preprint arXiv:1706.02677*, 2017.
- Han, S., Mao, H., and Dally, W. J. Deep compression: Compressing deep neural networks with pruning, trained quantization and huffman coding. *arXiv preprint arXiv:1510.00149*, 2015.
- He, H., Huang, G., and Yuan, Y. Asymmetric valleys: Beyond sharp and flat local minima. In *Advances in Neural Information Processing Systems*, pp. 2549–2560, 2019.
- Hein, M. and Andriushchenko, M. Formal guarantees on the robustness of a classifier against adversarial manipulation. In *Advances in Neural Information Processing Systems (NIPS)*, pp. 2266–2276, 2017.
- Hoffer, E., Hubara, I., and Soudry, D. Train longer, generalize better: closing the generalization gap in large batch training of neural networks. In *Advances in Neural Information Processing Systems*, pp. 1731–1741, 2017.
- Huang, P.-S., Stanforth, R., Welbl, J., Dyer, C., Yogatama, D., Gowal, S., Dvijotham, K., and Kohli, P. Achieving verified robustness to symbol substitutions via interval bound propagation. In *Proceedings of the 2019 Conference on Empirical Methods in Natural Language Processing and the 9th International Joint Conference on Natural Language Processing (EMNLP-IJCNLP)*, pp. 4074–4084, 2019.
- Jastrzebski, S., Kenton, Z., Arpit, D., Ballas, N., Fischer, A., Bengio, Y., and Storkey, A. J. Finding flatter minima with sgd. In *ICLR (Workshop)*, 2018.
- Jia, R., Raghunathan, A., Göksel, K., and Liang, P. Certified robustness to adversarial word substitutions. In *Proceedings of the 2019 Conference on Empirical Methods in Natural Language Processing and the 9th International Joint Conference on Natural Language Processing (EMNLP-IJCNLP)*, pp. 4120–4133, 2019.
- Julian, K. D., Sharma, S., Jeannin, J.-B., and Kochenderfer, M. J. Verifying aircraft collision avoidance neural networks through linear approximations of safe regions. *arXiv preprint arXiv:1903.00762*, 2019.
- Katz, G., Barrett, C., Dill, D. L., Julian, K., and Kochenderfer, M. J. Reluplex: An efficient smt solver for verifying deep neural networks. In *International Conference on Computer Aided Verification*, pp. 97–117. Springer, 2017.
- Keskar, N. S., Mudigere, D., Nocedal, J., Smelyanskiy, M., and Tang, P. T. P. On large-batch training for deep learning: Generalization gap and sharp minima. *arXiv preprint arXiv:1609.04836*, 2016.

- Kingma, D. P. and Ba, J. Adam: A method for stochastic optimization. *arXiv preprint arXiv:1412.6980*, 2014.
- Ko, C.-Y., Lyu, Z., Weng, T.-W., Daniel, L., Wong, N., and Lin, D. Popqorn: Quantifying robustness of recurrent neural networks. In *International Conference on Machine Learning*, pp. 3468–3477, 2019.
- Lyu, Z., Ko, C.-Y., Kong, Z., Wong, N., Lin, D., and Daniel, L. Fastened crown: Tightened neural network robustness certificates. *arXiv preprint arXiv:1912.00574*, 2019.
- Maurer, J., Singh, G., Mirman, M., Gehr, T., Hoffmann, A., Tsankov, P., Cohen, D. D., and Püschel, M. Eran user manual. 2018.
- Mirman, M., Gehr, T., and Vechev, M. Differentiable abstract interpretation for provably robust neural networks. In *International Conference on Machine Learning*, pp. 3575–3583, 2018.
- Paszke, A., Gross, S., Massa, F., Lerer, A., Bradbury, J., Chanan, G., Killeen, T., Lin, Z., Gimelshein, N., Antiga, L., Desmaison, A., Kopf, A., Yang, E., DeVito, Z., Raison, M., Tejani, A., Chilamkurthy, S., Steiner, B., Fang, L., Bai, J., and Chintala, S. Pytorch: An imperative style, high-performance deep learning library. In *Advances in Neural Information Processing Systems 32*, pp. 8024–8035. Curran Associates, Inc., 2019.
- Raghunathan, A., Steinhardt, J., and Liang, P. S. Semidefinite relaxations for certifying robustness to adversarial examples. In *Advances in Neural Information Processing Systems*, pp. 10877–10887, 2018.
- Rumelhart, D. E., Hinton, G. E., and Williams, R. J. Learning representations by back-propagating errors. *nature*, 323(6088):533–536, 1986.
- Salman, H., Yang, G., Zhang, H., Hsieh, C.-J., and Zhang, P. A convex relaxation barrier to tight robustness verification of neural networks. In *Advances in Neural Information Processing Systems 32*, pp. 9832–9842, 2019.
- Shi, Z., Zhang, H., Chang, K.-W., Huang, M., and Hsieh, C.-J. Robustness verification for transformers. In *International Conference on Learning Representations*, 2020.
- Singh, G., Gehr, T., Mirman, M., Püschel, M., and Vechev, M. Fast and effective robustness certification. In *Advances in Neural Information Processing Systems*, pp. 10825–10836, 2018.
- Singh, G., Ganvir, R., Püschel, M., and Vechev, M. Beyond the single neuron convex barrier for neural network certification. In *Advances in Neural Information Processing Systems*, pp. 15072–15083, 2019a.
- Singh, G., Gehr, T., Püschel, M., and Vechev, M. An abstract domain for certifying neural networks. *Proceedings of the ACM on Programming Languages*, 3(POPL):41, 2019b.
- Socher, R., Perelygin, A., Wu, J., Chuang, J., Manning, C. D., Ng, A., and Potts, C. Recursive deep models for semantic compositionality over a sentiment treebank. In *Proceedings of the 2013 conference on empirical methods in natural language processing*, pp. 1631–1642, 2013.
- Tjeng, V., Xiao, K., and Tedrake, R. Evaluating robustness of neural networks with mixed integer programming. *ICLR*, 2019.
- Vaswani, A., Shazeer, N., Parmar, N., Uszkoreit, J., Jones, L., Gomez, A. N., Kaiser, L., and Polosukhin, I. Attention is all you need. In *Advances in neural information processing systems*, pp. 5998–6008, 2017.
- Wang, S., Chen, Y., Abdou, A., and Jana, S. Mixtrain: Scalable training of formally robust neural networks. *arXiv preprint arXiv:1811.02625*, 2018a.
- Wang, S., Pei, K., Whitehouse, J., Yang, J., and Jana, S. Efficient formal safety analysis of neural networks. In *Advances in Neural Information Processing Systems*, pp. 6367–6377, 2018b.
- Wang, Y., Jha, S., and Chaudhuri, K. Analyzing the robustness of nearest neighbors to adversarial examples. In *International Conference on Machine Learning*, pp. 5120–5129, 2018c.

- Weng, T.-W., Zhang, H., Chen, H., Song, Z., Hsieh, C.-J., Daniel, L., Boning, D., and Dhillon, I. Towards fast computation of certified robustness for relu networks. In *International Conference on Machine Learning*, pp. 5273–5282, 2018.
- Wong, E. and Kolter, J. Z. Provable defenses against adversarial examples via the convex outer adversarial polytope. In *ICML*, 2018a.
- Wong, E. and Kolter, Z. Provable defenses against adversarial examples via the convex outer adversarial polytope. In *International Conference on Machine Learning*, pp. 5283–5292, 2018b.
- Wong, E., Schmidt, F., Metzen, J. H., and Kolter, J. Z. Scaling provable adversarial defenses. In *NIPS*, 2018.
- Xu, K., Chen, H., Liu, S., Chen, P.-Y., Weng, T.-W., Hong, M., and Lin, X. Topology attack and defense for graph neural networks: An optimization perspective. In *International Joint Conference on Artificial Intelligence (IJCAI)*, 2019a.
- Xu, K., Liu, S., Zhao, P., Chen, P.-Y., Zhang, H., Fan, Q., Erdogmus, D., Wang, Y., and Lin, X. Structured adversarial attack: Towards general implementation and better interpretability. In *International Conference on Learning Representations*, 2019b.
- Zhang, H., Weng, T.-W., Chen, P.-Y., Hsieh, C.-J., and Daniel, L. Efficient neural network robustness certification with general activation functions. In *Advances in neural information processing systems*, pp. 4939–4948, 2018.
- Zhang, H., Chen, H., Xiao, C., Li, B., Boning, D., and Hsieh, C.-J. Towards stable and efficient training of verifiably robust neural networks. *arXiv preprint arXiv:1906.06316*, 2019a.
- Zhang, H., Cheng, M., and Hsieh, C.-J. Enhancing certifiable robustness via a deep model ensemble. *arXiv preprint arXiv:1910.14655*, 2019b.
- Zhang, H., Zhang, P., and Hsieh, C.-J. Recurjac: An efficient recursive algorithm for bounding jacobian matrix of neural networks and its applications. *AAAI Conference on Artificial Intelligence*, 2019c.
- Zügner, D. and Günnemann, S. Certifiable robustness and robust training for graph convolutional networks. In *Proceedings of the 25th ACM SIGKDD International Conference on Knowledge Discovery & Data Mining*, pp. 246–256, 2019.

A Linear Bound Propagation for Activation Functions and Dot Products

In this section, we review how linear bound propagation for activation functions and dot product mentioned in Sec. 3.2 are performed, as proposed by previous works (Zhang et al., 2018; Shi et al., 2020).

Activation functions We assume that node v_i is computed from v_j with an activation function, i.e., $h_i(\mathbf{X}) = \sigma(h_j(\mathbf{X}))$. With the concretized bounds of $h_j(\mathbf{X})$, i.e., \underline{h}_j and \bar{h}_j computed previously, $\sigma(h_j(\mathbf{X}))$ can be linearly relaxed as

$$\underline{\mathbf{D}}h_j(\mathbf{X}) + \underline{\mathbf{c}} \leq \sigma(h_j(\mathbf{X})) \leq \bar{\mathbf{D}}h_j(\mathbf{X}) + \bar{\mathbf{c}}, \forall \underline{h}_j \leq h_j(\mathbf{X}) \leq \bar{h}_j, \quad (14)$$

where $h_j(\mathbf{X})$ is a vector and the inequality here is element-wise for the vectors. And we denote the t -th dimension of vector $h_j(\mathbf{X})$ as $[h_j(\mathbf{X})]_t$, the t -th dimension of $\sigma(h_j(\mathbf{X}))$ as $[\sigma(h_j(\mathbf{X}))]_t$, and similarly for other vectors. For $[h_j(\mathbf{X})]_t$, we actually aim to find a line with slope α_t and y-intercept β_t such that :

$$\underline{\alpha}_t[h_j(\mathbf{X})]_t + \underline{\beta}_t \leq [\sigma(h_j(\mathbf{X}))]_t \leq \bar{\alpha}_t[h_j(\mathbf{X})]_t + \bar{\beta}_t, \quad \forall [\underline{h}_j]_t \leq [h_j(\mathbf{X})]_t \leq [\bar{h}_j]_t,$$

and thereby

$$\underline{\mathbf{D}}_t = \underline{\alpha}_t \mathbf{e}_t, \quad \underline{\mathbf{c}}_t = \underline{\beta}_t, \quad \bar{\mathbf{D}}_t = \bar{\alpha}_t \mathbf{e}_t, \quad \bar{\mathbf{c}}_t = \bar{\beta}_t,$$

where \mathbf{e}_t is a standard unit vector at the t -th coordinate.

Activation functions involved in this work include ReLU tanh, sigmoid, and also element-wise nonlinear functions that can also be treated as activation functions, such as exp in softmax. We review the linear relaxation of ReLU, tanh and sigmoid as examples, and refer readers to Shi et al. (2020) for other element-wise nonlinear functions involved in Transformers.

For **ReLU**, $[\sigma(h_j(\mathbf{X}))]_t = \max([h_j(\mathbf{X})]_t, 0)$, it is already a linear function on segments $[h_j(\mathbf{X})]_t \in (-\infty, 0]$ and $[h_j(\mathbf{X})]_t \in [0, \infty)$ respectively. Therefore, when $[\bar{h}_j]_t \leq 0$ holds true, we make

$$\underline{\alpha}_t = \bar{\alpha}_t = \underline{\beta}_t = \bar{\beta}_t = 0,$$

since $[\sigma(h_j(\mathbf{X}))]_t \equiv 0$ holds true for $[h_j(\mathbf{X})]_t \leq [\bar{h}_j]_t \leq 0$. And when $[\underline{h}_j]_t \geq 0$ holds true, we make

$$\underline{\alpha}_t = \bar{\alpha}_t = 1, \quad \underline{\beta}_t = \bar{\beta}_t = 0,$$

since $[\sigma(h_j(\mathbf{X}))]_t = [h_j(\mathbf{X})]_t$ holds true for $[h_j(\mathbf{X})]_t \geq [\underline{h}_j]_t \geq 0$. Moreover, when $[\underline{h}_j]_t < 0 < [\bar{h}_j]_t$, $[\sigma(h_j(\mathbf{X}))]_t$ is not a linear function within the range of $[h_j(\mathbf{X})]_t$, and thus we perform a non-trivial linear relaxation. For the upper bound, we make it the line passing *endpoints* $([\underline{h}_j]_t, [\sigma(\underline{h}_j)]_t)$ and $([\bar{h}_j]_t, [\sigma(\bar{h}_j)]_t)$:

$$\bar{\alpha}_t = \frac{[\sigma(\bar{h}_j)]_t - [\sigma(\underline{h}_j)]_t}{[\bar{h}_j]_t - [\underline{h}_j]_t}, \quad \bar{\beta}_t = 0. \quad (15)$$

For the lower bound, we take:

$$\begin{cases} \underline{\alpha}_t = 0, \quad \underline{\beta}_t = 0 & [\bar{h}_j]_t < |[\underline{h}_j]_t| \\ \underline{\alpha}_t = 1, \quad \underline{\beta}_t = 0 & [\bar{h}_j]_t \geq |[\underline{h}_j]_t| \end{cases}.$$

For **tanh**,

$$[\sigma(h_j(\mathbf{X}))]_t = \frac{1 - e^{-2[h_j(\mathbf{X})]_t}}{1 + e^{-2[h_j(\mathbf{X})]_t}},$$

it is concave on $[h_j(\mathbf{X})]_t > 0$ while convex on $[h_j(\mathbf{X})]_t < 0$. When $[\underline{h}_j]_t \geq 0$ holds true, the function is completely concave within the range of $[h_j(\mathbf{X})]_t$, and thus we take the line passing the two endpoints as the lower bound, similarly as Eq. (15) but we make it the lower bound rather than the upper bound here, and we take the tangent line passing

$$p_t = \left(\frac{[\underline{h}_j]_t + [\bar{h}_j]_t}{2}, \sigma\left(\frac{[\underline{h}_j]_t + [\bar{h}_j]_t}{2}\right) \right)$$

as the lower bound, whose slope and y-intercept can be easily computed. When $[\bar{h}_j]_t \leq 0$ holds true, the function is completely convex within the range of $[h_j(\mathbf{X})]_t$, and thus we take the line passing the two endpoints as the upper bound and take the tangent line passing p_t as the lower bound. Besides, when $[h_j]_t < 0 < [\bar{h}_j]_t$, we take a tangent line passing the right endpoint as the lower bound, and take a tangent line passing the left endpoint as the upper bound, where the tangent points other than the endpoints can be found via binary search. Moreover, **sigmoid** has a similar property as tanh and the method for linear relaxation described above also applies to sigmoid.

In the bound propagation for activation functions, for the forward mode perturbation analysis with function F_i , the bound of $h_j(\mathbf{X})$ is:

$$\underline{\mathbf{A}}^{(j)}\mathbf{X} + \underline{\mathbf{b}}^{(j)} \leq h_j(\mathbf{X}) \leq \overline{\mathbf{A}}^{(j)}\mathbf{X} + \overline{\mathbf{b}}^{(j)},$$

and with Eq. (14), we have

$$\begin{aligned} & \underline{\mathbf{D}}_+(\underline{\mathbf{A}}^{(j)}\mathbf{X} + \underline{\mathbf{b}}^{(j)}) + \underline{\mathbf{D}}_-(\overline{\mathbf{A}}^{(j)}\mathbf{X} + \overline{\mathbf{b}}^{(j)}) + \underline{\mathbf{c}} \\ & \leq h_i(\mathbf{X}) = \sigma(h_j(\mathbf{X})) \\ & \leq \overline{\mathbf{D}}_+(\overline{\mathbf{A}}^{(j)}\mathbf{X} + \overline{\mathbf{b}}^{(j)}) + \overline{\mathbf{D}}_-(\underline{\mathbf{A}}^{(j)}\mathbf{X} + \underline{\mathbf{b}}^{(j)}) + \overline{\mathbf{c}}, \end{aligned}$$

and thus

$$\underline{\mathbf{A}}^{(i)}\mathbf{X} + \underline{\mathbf{b}}^{(i)} \leq h_i(\mathbf{X}) \leq \overline{\mathbf{A}}^{(i)}\mathbf{X} + \overline{\mathbf{b}}^{(i)},$$

where

$$\begin{aligned} \underline{\mathbf{A}}^{(i)} &= \underline{\mathbf{D}}_+\underline{\mathbf{A}}^{(j)} + \underline{\mathbf{D}}_-\overline{\mathbf{A}}^{(j)}, \underline{\mathbf{b}}^{(i)} = \underline{\mathbf{D}}_+\underline{\mathbf{b}}^{(j)} + \underline{\mathbf{D}}_-\overline{\mathbf{b}}^{(j)} + \underline{\mathbf{c}}, \\ \overline{\mathbf{A}}^{(i)} &= \overline{\mathbf{D}}_+\overline{\mathbf{A}}^{(j)} + \overline{\mathbf{D}}_-\underline{\mathbf{A}}^{(j)}, \overline{\mathbf{b}}^{(i)} = \overline{\mathbf{D}}_+\overline{\mathbf{b}}^{(j)} + \overline{\mathbf{D}}_-\underline{\mathbf{b}}^{(j)} + \overline{\mathbf{c}}. \end{aligned}$$

For the bound propagation in the backward mode perturbation analysis, when we are computing the linear bounds of $h_k(\mathbf{X})$, there are terms regarding $h_i(\mathbf{X})$, are $\hat{\underline{\mathbf{A}}}^{(k,i)}h_i(\mathbf{X})$ and $\hat{\overline{\mathbf{A}}}^{(k,i)}h_i(\mathbf{X})$. By substituting $h_i(\mathbf{X}) = \sigma(h_j(\mathbf{X}))$ with Eq.(14), we have

$$\begin{aligned} \hat{\underline{\mathbf{A}}}^{(k,i)}h_i(\mathbf{X}) &\geq \hat{\underline{\mathbf{A}}}_+^{(k,i)}(\underline{\mathbf{D}}h_j(\mathbf{X}) + \underline{\mathbf{c}}) + \hat{\underline{\mathbf{A}}}_-^{(k,i)}(\overline{\mathbf{D}}h_j(\mathbf{X}) + \overline{\mathbf{c}}), \\ \hat{\overline{\mathbf{A}}}^{(k,i)}h_i(\mathbf{X}) &\leq \hat{\overline{\mathbf{A}}}_+^{(k,i)}(\overline{\mathbf{D}}h_j(\mathbf{X}) + \overline{\mathbf{c}}) + \hat{\overline{\mathbf{A}}}_-^{(k,i)}(\underline{\mathbf{D}}h_j(\mathbf{X}) + \underline{\mathbf{c}}). \end{aligned}$$

By merging the coefficients of $h_j(\mathbf{X})$ and the bias terms, we have

$$\hat{\underline{\mathbf{A}}}^{(k,i)}h_i(\mathbf{X}) \geq \hat{\underline{\mathbf{A}}}^{(k,i,j)}h_j(\mathbf{X}) + \hat{\underline{\mathbf{b}}}^{(k,i,j)}, \quad \hat{\overline{\mathbf{A}}}^{(k,i)}h_i(\mathbf{X}) \leq \hat{\overline{\mathbf{A}}}^{(k,i,j)}h_j(\mathbf{X}) + \hat{\overline{\mathbf{b}}}^{(k,i,j)},$$

where

$$\begin{aligned} \hat{\underline{\mathbf{A}}}^{(k,i,j)} &= \hat{\underline{\mathbf{A}}}_+^{(k,i)} \cdot \underline{\mathbf{D}} + \hat{\underline{\mathbf{A}}}_-^{(k,i)} \cdot \overline{\mathbf{D}}, & \hat{\underline{\mathbf{b}}}^{(k,i,j)} &= \hat{\underline{\mathbf{A}}}_+^{(k,i)} \cdot \underline{\mathbf{c}} + \hat{\underline{\mathbf{A}}}_-^{(k,i)} \cdot \overline{\mathbf{c}}, \\ \hat{\overline{\mathbf{A}}}^{(k,i,j)} &= \hat{\overline{\mathbf{A}}}_+^{(k,i)} \cdot \overline{\mathbf{D}} + \hat{\overline{\mathbf{A}}}_-^{(k,i)} \cdot \underline{\mathbf{D}}, & \hat{\overline{\mathbf{b}}}^{(k,i,j)} &= \hat{\overline{\mathbf{A}}}_+^{(k,i)} \cdot \overline{\mathbf{c}} + \hat{\overline{\mathbf{A}}}_-^{(k,i)} \cdot \underline{\mathbf{c}}. \end{aligned}$$

Dot product Dot product is an essential operation in the self-attention mechanism of Transformers. We assume that node v_i is computed from taking the dot product of v_p and v_q . Although in the most places of this paper, we regard $h_i(\mathbf{X}), h_p(\mathbf{X}), h_q(\mathbf{X})$ as flattened vectors, they are tensors in practice and we can actually view them as 2-dimensional matrices when they are not flattened. We denote the element at the s -th row and the t -th column of $h_i(\mathbf{X})$ as $[h_i(\mathbf{X})]_{s,t}$, and this notation also applies to other matrices. The dot product operation here is defined by

$$h_i(\mathbf{X}) = h_p(\mathbf{X})h_q(\mathbf{X})^\top,$$

where

$$[h_i(\mathbf{X})]_{s,t} = \sum_r [h_p(\mathbf{X})]_{s,r} [h_q(\mathbf{X})]_{t,r}. \quad (16)$$

Following Shi et al. (2020), each multiplication in Eq. (16) can be linearly relaxed as

$$\underline{\alpha}_{r,s,t}[h_p(\mathbf{X})]_{s,r} + \underline{\beta}_{r,s,t}[h_q(\mathbf{X})]_{t,r} + \underline{\gamma}_{r,s,t} \leq [h_p(\mathbf{X})]_{s,r}[h_q(\mathbf{X})]_{t,r} \leq \bar{\alpha}_{r,s,t}[h_p(\mathbf{X})]_{s,r} + \bar{\beta}_{r,s,t}[h_q(\mathbf{X})]_{t,r} + \bar{\gamma}_{r,s,t},$$

where the parameters for linear relaxation, $\underline{\alpha}_{r,s,t}$, $\underline{\beta}_{r,s,t}$, $\underline{\gamma}_{r,s,t}$, $\bar{\alpha}_{r,s,t}$, $\bar{\beta}_{r,s,t}$, $\bar{\gamma}_{r,s,t}$ are as follows:

$$\begin{aligned}\underline{\alpha}_{r,s,t} &= [h_q(\mathbf{X})]_{t,r}, \bar{\alpha}_{r,s,t} = [\bar{h}_q(\mathbf{X})]_{t,r}, \\ \underline{\beta}_{r,s,t} &= \bar{\beta}_{r,s,t} = [h_p(\mathbf{X})]_{s,r}, \\ \underline{\gamma}_{r,s,t} &= -\underline{\alpha}_{r,s,t}\underline{\beta}_{r,s,t}, \bar{\gamma}_{r,s,t} = -\bar{\alpha}_{r,s,t}\bar{\beta}_{r,s,t}.\end{aligned}$$

Therefore,

$$\sum_r \underline{\alpha}_{r,s,t}[h_p(\mathbf{X})]_{s,r} + \underline{\beta}_{r,s,t}[h_q(\mathbf{X})]_{t,r} + \underline{\gamma}_{r,s,t} \leq [h_i(\mathbf{X})]_{s,t} \leq \sum_r \bar{\alpha}_{r,s,t}[h_p(\mathbf{X})]_{s,r} + \bar{\beta}_{r,s,t}[h_q(\mathbf{X})]_{t,r} + \bar{\gamma}_{r,s,t}. \quad (17)$$

We refer readers to Shi et al. (2020) for a proof.

Thereby, in the forward mode perturbation analysis, for F_i :

$$\begin{aligned}\underline{\mathbf{A}}_{(s,t)}^{(i)} &= \sum_r \{ \underline{\alpha}_{r,s,t}(\mathbf{I}(\underline{\alpha}_{r,s,t} > 0)\underline{\mathbf{A}}_{(s,r)}^{(p)} + \mathbf{I}(\underline{\alpha}_{r,s,t} < 0)\bar{\mathbf{A}}_{(s,r)}^{(p)}) + \underline{\beta}_{r,s,t}(\mathbf{I}(\underline{\beta}_{r,s,t} > 0)\underline{\mathbf{A}}_{(t,r)}^{(q)} + \mathbf{I}(\underline{\beta}_{r,s,t} < 0)\bar{\mathbf{A}}_{(t,r)}^{(q)}) \}, \\ \underline{\mathbf{b}}_{(s,t)}^{(i)} &= \sum_r \{ \underline{\gamma}_{r,s,t} + \underline{\alpha}_{r,s,t}(\mathbf{I}(\underline{\alpha}_{r,s,t} > 0)\underline{\mathbf{b}}_{(s,r)}^{(p)} + \mathbf{I}(\underline{\alpha}_{r,s,t} < 0)\bar{\mathbf{b}}_{(s,r)}^{(p)}) + \underline{\beta}_{r,s,t}(\mathbf{I}(\underline{\beta}_{r,s,t} > 0)\underline{\mathbf{b}}_{(t,r)}^{(q)} + \mathbf{I}(\underline{\beta}_{r,s,t} < 0)\bar{\mathbf{b}}_{(t,r)}^{(q)}) \}, \\ \bar{\mathbf{A}}_{(s,t)}^{(i)} &= \sum_r \{ \bar{\alpha}_{r,s,t}(\mathbf{I}(\bar{\alpha}_{r,s,t} > 0)\bar{\mathbf{A}}_{(s,r)}^{(p)} + \mathbf{I}(\bar{\alpha}_{r,s,t} < 0)\underline{\mathbf{A}}_{(s,r)}^{(p)}) + \bar{\beta}_{r,s,t}(\mathbf{I}(\bar{\beta}_{r,s,t} > 0)\bar{\mathbf{A}}_{(t,r)}^{(q)} + \mathbf{I}(\bar{\beta}_{r,s,t} < 0)\underline{\mathbf{A}}_{(t,r)}^{(q)}) \}, \\ \bar{\mathbf{b}}_{(s,t)}^{(i)} &= \sum_r \{ \bar{\gamma}_{r,s,t} + \bar{\alpha}_{r,s,t}(\mathbf{I}(\bar{\alpha}_{r,s,t} > 0)\bar{\mathbf{b}}_{(s,r)}^{(p)} + \mathbf{I}(\bar{\alpha}_{r,s,t} < 0)\underline{\mathbf{b}}_{(s,r)}^{(p)}) + \bar{\beta}_{r,s,t}(\mathbf{I}(\bar{\beta}_{r,s,t} > 0)\bar{\mathbf{b}}_{(t,r)}^{(q)} + \mathbf{I}(\bar{\beta}_{r,s,t} < 0)\underline{\mathbf{b}}_{(t,r)}^{(q)}) \},\end{aligned}$$

where $\underline{\mathbf{A}}_{(s,t)}^{(i)}$ denotes a row in matrix $\underline{\mathbf{A}}^{(i)}$ and $\underline{\mathbf{b}}_{(s,t)}^{(i)}$ denotes a dimension in vector $\underline{\mathbf{b}}^{(i)}$ that corresponds to the parameters for the linear lower bound of $[h_i(\mathbf{X})]_{s,t}$ respectively, which is also similar for other parameters $\bar{\mathbf{A}}_{(s,t)}^{(i)}$, $\underline{\mathbf{A}}_{(s,r)}^{(p)}$, $\bar{\mathbf{A}}_{(s,r)}^{(p)}$, $\underline{\mathbf{A}}_{(t,r)}^{(q)}$, $\bar{\mathbf{A}}_{(t,r)}^{(q)}$, $\underline{\mathbf{b}}_{(s,t)}^{(p)}$, $\bar{\mathbf{b}}_{(s,t)}^{(p)}$, $\underline{\mathbf{b}}_{(s,r)}^{(p)}$, $\bar{\mathbf{b}}_{(s,r)}^{(p)}$, $\underline{\mathbf{b}}_{(t,r)}^{(q)}$, $\bar{\mathbf{b}}_{(t,r)}^{(q)}$.

In the backward mode perturbation analysis, when we are representing the bounds of $h_k(\mathbf{X})$, there are terms in the linear bounds regarding $[h_i(\mathbf{X})]_{s,t}$, $\hat{\underline{\mathbf{A}}}_{:, (s,t)}^{(k,i)}[h_i(\mathbf{X})]_{s,t}$ and $\bar{\hat{\mathbf{A}}}_{:, (s,t)}^{(k,i)}[h_i(\mathbf{X})]_{s,t}$, where $\hat{\underline{\mathbf{A}}}_{:, (s,t)}^{(k,i)}$ and $\bar{\hat{\mathbf{A}}}_{:, (s,t)}^{(k,i)}$ represent the column corresponding to the coefficients of $[h_i(\mathbf{X})]_{s,t}$ in $\hat{\underline{\mathbf{A}}}^{(k,i)}$ and $\bar{\hat{\mathbf{A}}}^{(k,i)}$ respectively. By substituting $[h_i(\mathbf{X})]_{s,t}$ with Eq. (17), we have

$$\begin{aligned}\hat{\underline{\mathbf{A}}}_{:, (s,t)}^{(k,i)}[h_i(\mathbf{X})]_{s,t} &\geq \hat{\underline{\mathbf{A}}}_{:, (s,t),+}^{(k,i)} \left(\sum_r \underline{\alpha}_{r,s,t}[h_p(\mathbf{X})]_{s,r} + \underline{\beta}_{r,s,t}[h_q(\mathbf{X})]_{t,r} + \underline{\gamma}_{r,s,t} \right) + \hat{\underline{\mathbf{A}}}_{:, (s,t),-}^{(k,i)} \left(-\sum_r \bar{\alpha}_{r,s,t}[h_p(\mathbf{X})]_{s,r} + \bar{\beta}_{r,s,t}[h_q(\mathbf{X})]_{t,r} + \bar{\gamma}_{r,s,t} \right), \\ \bar{\hat{\mathbf{A}}}_{:, (s,t)}^{(k,i)}[h_i(\mathbf{X})]_{s,t} &\leq \bar{\hat{\mathbf{A}}}_{:, (s,t),+}^{(k,i)} \left(\sum_r \bar{\alpha}_{r,s,t}[h_p(\mathbf{X})]_{s,r} + \bar{\beta}_{r,s,t}[h_q(\mathbf{X})]_{t,r} + \bar{\gamma}_{r,s,t} \right) + \bar{\hat{\mathbf{A}}}_{:, (s,t),-}^{(k,i)} \left(-\sum_r \underline{\alpha}_{r,s,t}[h_p(\mathbf{X})]_{s,r} + \underline{\beta}_{r,s,t}[h_q(\mathbf{X})]_{t,r} + \underline{\gamma}_{r,s,t} \right),\end{aligned}$$

where $\hat{\underline{\mathbf{A}}}_{:, (s,t),+}^{(k,i)}$ and $\hat{\underline{\mathbf{A}}}_{:, (s,t),-}^{(k,i)}$ stand for retaining positive and negative elements from $\hat{\underline{\mathbf{A}}}_{:, (s,t)}^{(k,i)}$ respectively, which is also similar for $\bar{\hat{\mathbf{A}}}_{:, (s,t),+}^{(k,i)}$ and $\bar{\hat{\mathbf{A}}}_{:, (s,t),-}^{(k,i)}$. This is equivalent to

$$\begin{aligned}\hat{\underline{\mathbf{A}}}_{:, (s,t)}^{(k,i)}[h_i(\mathbf{X})]_{s,t} &\geq \sum_r \{ (\underline{\alpha}_{r,s,t}\hat{\underline{\mathbf{A}}}_{:, (s,t),+}^{(k,i)} + \bar{\alpha}_{r,s,t}\hat{\underline{\mathbf{A}}}_{:, (s,t),-}^{(k,i)})[h_p(\mathbf{X})]_{s,r} + (\underline{\beta}_{r,s,t}\hat{\underline{\mathbf{A}}}_{:, (s,t),+}^{(k,i)} + \bar{\beta}_{r,s,t}\hat{\underline{\mathbf{A}}}_{:, (s,t),-}^{(k,i)})[h_q(\mathbf{X})]_{t,r} + \underline{\gamma}_{r,s,t}\hat{\underline{\mathbf{A}}}_{:, (s,t),+}^{(k,i)} + \bar{\gamma}_{r,s,t}\hat{\underline{\mathbf{A}}}_{:, (s,t),-}^{(k,i)} \}, \\ \bar{\hat{\mathbf{A}}}_{:, (s,t)}^{(k,i)}[h_i(\mathbf{X})]_{s,t} &\leq \sum_r \{ (\bar{\alpha}_{r,s,t}\bar{\hat{\mathbf{A}}}_{:, (s,t),+}^{(k,i)} + \underline{\alpha}_{r,s,t}\bar{\hat{\mathbf{A}}}_{:, (s,t),-}^{(k,i)})[h_p(\mathbf{X})]_{s,r} + (\bar{\beta}_{r,s,t}\bar{\hat{\mathbf{A}}}_{:, (s,t),+}^{(k,i)} + \underline{\beta}_{r,s,t}\bar{\hat{\mathbf{A}}}_{:, (s,t),-}^{(k,i)})[h_q(\mathbf{X})]_{t,r} + \bar{\gamma}_{r,s,t}\bar{\hat{\mathbf{A}}}_{:, (s,t),+}^{(k,i)} + \underline{\gamma}_{r,s,t}\bar{\hat{\mathbf{A}}}_{:, (s,t),-}^{(k,i)} \}.\end{aligned}$$

By considering all the possible $[h_i(\mathbf{X})]_{s,t}$ in $h_i(\mathbf{X})$ and merging the coefficient terms of the corresponding $[h_p(\mathbf{X})]_{s,r}$, $[h_q(\mathbf{X})]_{t,r}$ and also the bias terms, we have

$$\begin{aligned} \sum_{(s,t)} \hat{\mathbf{A}}_{:, (s,t)}^{(k,i)} [h_i(\mathbf{X})]_{s,t} &\geq \sum_{(s,t)} \sum_r (\hat{\mathbf{A}}_{:, (s,r)}^{(k,i,p)} [h_p(\mathbf{X})]_{s,r} + \hat{\mathbf{A}}_{:, (t,r)}^{(k,i,q)} [h_q(\mathbf{X})]_{t,r}) + \hat{\mathbf{b}}^{(k,i)}, \\ \sum_{(s,t)} \overline{\mathbf{A}}_{:, (s,t)}^{(k,i)} [h_i(\mathbf{X})]_{s,t} &\leq \sum_{(s,t)} \sum_r (\overline{\mathbf{A}}_{:, (s,r)}^{(k,i,p)} [h_p(\mathbf{X})]_{s,r} + \overline{\mathbf{A}}_{:, (t,r)}^{(k,i,q)} [h_q(\mathbf{X})]_{t,r}) + \overline{\mathbf{b}}^{(k,i)}, \end{aligned}$$

where

$$\begin{aligned} \hat{\mathbf{A}}_{:, (s,r)}^{(k,i,p)} &= \sum_t \underline{\alpha}_{r,s,t} \hat{\mathbf{A}}_{:, (s,t),+}^{(k,i)} + \overline{\alpha}_{r,s,t} \hat{\mathbf{A}}_{:, (s,t),-}^{(k,i)}, \\ \hat{\mathbf{A}}_{:, (t,r)}^{(k,i,q)} &= \sum_s \underline{\beta}_{r,s,t} \hat{\mathbf{A}}_{:, (s,t),+}^{(k,i)} + \overline{\beta}_{r,s,t} \hat{\mathbf{A}}_{:, (s,t),-}^{(k,i)}, \\ \hat{\mathbf{b}}^{(k,i)} &= \sum_{(s,t)} \sum_r \underline{\gamma}_{r,s,t} \hat{\mathbf{A}}_{:, (s,t),+}^{(k,i)} + \overline{\gamma}_{r,s,t} \hat{\mathbf{A}}_{:, (s,t),-}^{(k,i)}, \\ \overline{\mathbf{A}}_{:, (s,r)}^{(k,i,p)} &= \sum_t \overline{\alpha}_{r,s,t} \overline{\mathbf{A}}_{:, (s,t),+}^{(k,i)} + \underline{\alpha}_{r,s,t} \overline{\mathbf{A}}_{:, (s,t),-}^{(k,i)}, \\ \overline{\mathbf{A}}_{:, (t,r)}^{(k,i,q)} &= \sum_s \overline{\beta}_{r,s,t} \overline{\mathbf{A}}_{:, (s,t),+}^{(k,i)} + \underline{\beta}_{r,s,t} \overline{\mathbf{A}}_{:, (s,t),-}^{(k,i)}, \\ \overline{\mathbf{b}}^{(k,i)} &= \sum_{(s,t)} \sum_r \overline{\gamma}_{r,s,t} \overline{\mathbf{A}}_{:, (s,t),+}^{(k,i)} + \underline{\gamma}_{r,s,t} \overline{\mathbf{A}}_{:, (s,t),-}^{(k,i)}. \end{aligned}$$

jointly define G_i .

Dot product is also used in the weighted summation of hidden states after computing self-attention scores. In addition, Transformers and LSTM also involve element-wise multiplication or division, which can be achieved with a similar linear relaxation used for each multiplication of dot product. Again, we refer readers to Shi et al. (2020) for details.

B Proof of Theorem 1

In Theorem 1, we aim to represent the bounds of node v_k with linear functions of nodes that v_k is dependent on:

$$\sum_{i=1}^n \hat{\mathbf{A}}^{(k,i)} h_i(\mathbf{X}) + \hat{\mathbf{b}}^{(k)} \leq h_k(\mathbf{X}) \leq \sum_{i=1}^n \overline{\mathbf{A}}^{(k,i)} h_i(\mathbf{X}) + \overline{\mathbf{b}}^{(k)}, \quad (18)$$

where $\mathbf{X} \in \mathbb{S}$, $\hat{\mathbf{A}}^{(k,i)}$, $\hat{\mathbf{b}}^{(k)}$, $\overline{\mathbf{A}}^{(k,i)}$, $\overline{\mathbf{b}}^{(k)}$ are parameters, and $\hat{\mathbf{A}}^{(k,i)}$ and $\overline{\mathbf{A}}^{(k,i)}$ are zero matrices if v_k is not dependent on v_i .

Initially, this inequality holds true with

$$\begin{aligned} \hat{\mathbf{A}}^{(k,k)} &= \overline{\mathbf{A}}^{(k,k)} = \mathbf{I}, \quad \hat{\mathbf{A}}^{(k,i)} = \overline{\mathbf{A}}^{(k,i)} = \mathbf{0} \quad (\forall i \neq k), \\ \hat{\mathbf{b}}^{(k)} &= \overline{\mathbf{b}}^{(k)} = \mathbf{0}, \end{aligned}$$

because then

$$\sum_{i=1}^n \hat{\mathbf{A}}^{(k,i)} h_i(\mathbf{X}) + \hat{\mathbf{b}}^{(k)} = \sum_{i=1}^n \overline{\mathbf{A}}^{(k,i)} h_i(\mathbf{X}) + \overline{\mathbf{b}}^{(k)} = h_k(\mathbf{X})$$

meets Eq. (18).

Without loss of generality, we assume that the nodes are numbered in topological order, i.e., for each node v_i and its input node $u_{i,j}$, $v_i > u_{i,j}$ holds true, and all the independent nodes have the smallest numbers, which can be achieved via a topological sort for any computational graph. Assuming that there are n' independent nodes, in Theorem 1, we aim to propagate the parameters in Eq. (18), such that in the end $\hat{\mathbf{A}}^{(k,i)}$ and $\overline{\mathbf{A}}^{(k,i)}$

are non-zero only when $i \leq n'$, i.e., when v_i is an independent node, and thereby the bounds of $h_k(\mathbf{X})$ will be represented as linear functions of the values of independent nodes only.

We prove that this goal can be achieved. We assume that v_t is the largest-numbered node with non-zero $\hat{\mathbf{A}}^{(k,t)}$ or $\overline{\mathbf{A}}^{(k,t)}$. If $t \leq n'$, the goal is already achieved. Otherwise, by applying the G_t function as described in Sec. 3.2, terms $\hat{\mathbf{A}}^{(k,t)} h_t(\mathbf{X})$ and $\overline{\mathbf{A}}^{(k,t)} h_t(\mathbf{X})$ can be bounded by

$$\sum_{j=1}^{m_t} \hat{\mathbf{A}}^{(k,t,u_{t,j})} h_{u_{t,j}}(\mathbf{X}) + \hat{\mathbf{b}}^{(k,t)} \leq \hat{\mathbf{A}}^{(k,t)} h_t(\mathbf{X}), \quad (19)$$

$$\overline{\mathbf{A}}^{(k,t)} h_t(\mathbf{X}) \leq \sum_{j=1}^{m_t} \overline{\mathbf{A}}^{(k,t,u_{t,j})} h_{u_{t,j}}(\mathbf{X}) + \overline{\mathbf{b}}^{(k,t)}, \forall \mathbf{X} \in \mathbb{S} \quad (20)$$

respectively. We substitute $\hat{\mathbf{A}}^{(k,t)} h_t(\mathbf{X})$ in Eq. (18) with Eq. (19) and Eq. (20), yielding:

$$h_k(\mathbf{X}) \geq \sum_{i \neq t} \hat{\mathbf{A}}^{(k,i)} h_i(\mathbf{X}) + \sum_{j=1}^{m_t} \hat{\mathbf{A}}^{(k,t,u_{t,j})} h_{u_{t,j}}(\mathbf{X}) + \hat{\mathbf{b}}^{(k,t)} + \hat{\mathbf{b}}^{(k)} \quad (21)$$

$$h_k(\mathbf{X}) \leq \sum_{i \neq t} \overline{\mathbf{A}}^{(k,i)} h_i(\mathbf{X}) + \sum_{j=1}^{m_t} \overline{\mathbf{A}}^{(k,t,u_{t,j})} h_{u_{t,j}}(\mathbf{X}) + \overline{\mathbf{b}}^{(k,t)} + \overline{\mathbf{b}}^{(k)} \quad (22)$$

By merging $\hat{\mathbf{A}}^{(k,t,u_{t,j})}$ with $\hat{\mathbf{A}}^{(k,u_{t,j})}$ and merging $\overline{\mathbf{A}}^{(k,t,u_{t,j})}$ with $\overline{\mathbf{A}}^{(k,u_{t,j})}$, we propagate and update the parameters: we add $\hat{\mathbf{A}}^{(k,t,u_{t,j})}$ to $\hat{\mathbf{A}}^{(k,u_{t,j})}$, add $\overline{\mathbf{A}}^{(k,t,u_{t,j})}$ to $\overline{\mathbf{A}}^{(k,u_{t,j})}$, add $\hat{\mathbf{b}}^{(k,t)}$ to $\hat{\mathbf{b}}^{(k)}$, add $\overline{\mathbf{b}}^{(k,t)}$ to $\overline{\mathbf{b}}^{(k)}$, and also set $\hat{\mathbf{A}}^{(k,t)}$ and $\overline{\mathbf{A}}^{(k,t)}$ to $\mathbf{0}$, and the new parameters make Eq. (18) still hold true. Meanwhile, since $\hat{\mathbf{A}}^{(k,t)}$ and $\overline{\mathbf{A}}^{(k,t)}$ have been set to $\mathbf{0}$ and $u_{t,j} < t$ ($1 \leq j \leq m_t$), the current largest-numbered node $v_{t'}$ with non-zero $\hat{\mathbf{A}}^{(k,t')}$ or $\overline{\mathbf{A}}^{(k,t')}$ satisfies $t' \leq t - 1$, and then the new value of t can be updated to t' by definition. Therefore, as long as $t > n'$, by applying the G_t function, we can make t decrease by at least 1, and thus by repeating this process, we can finally make $t \leq n'$, and our goal can then be achieved.

C Complexity Comparison between the Forward Mode and the Backward Mode

In this section, we analyze the computational cost of four LiRPA variants for usual classification models: IBP \rightarrow backward, pure forward, forward \rightarrow backward and pure backward perturbation analysis.

We assume that D_x and D_y are the total dimension of the input and final output of the computational graph respectively. We focus on a usual case in classification models, where the final output node is a logits layer whose dimension equals to the number of classes and is thus usually small, i.e., $D_y \ll D_x$. We also assume that the time complexity of a regular forward pass of the computational graph (e.g., a regular inference pass) is $O(N)$, and there are M neurons in the graph (the total dimension of all the nodes).

The time complexity of pure IBP is still $O(N)$ since it computes two output values, a lower bound and an upper bound, for each neuron, and thus the time complexity is the same as a regular pass which computes one output value for each neuron. However, pure IBP cannot give tight enough bounds especially for models without robust training.

For IBP \rightarrow backward, we further compute the bounds of the final output layer with a backward bound propagation which computes $O(D_y)$ values for each neuron, and these values stand for the coefficients of the linear bounds of the final output neurons. Therefore, the total time complexity of IBP \rightarrow backward is $O(D_y N)$. For pure forward perturbation analysis, since we represent the bounds of each neuron with linear functions of the graph input, we need to compute $O(D_x)$ values for each neuron. Therefore, the time complexity of pure forward perturbation analysis is $O(D_x N)$. Forward \rightarrow backward further needs a backward propagation for the final output layer, and thus the total complexity is $O(D_x N + D_y N) \approx O(D_x N)$ when $D_y \ll D_x$. For pure backward perturbation analysis, we need to compute the bounds of all the intermediate nodes with

a backward propagation respectively. As a result, we need to compute $O(M)$ values for each neuron, and these values stand for the coefficients of linear bounds. These coefficients are needed either when we are representing the bounds of this neuron with linear functions of other nodes that it depends on, or we are representing the bounds of other neurons that depends on this neuron with linear functions, and thus there are $O(M)$ coefficients for each neuron. Therefore, the time complexity of pure backward perturbation analysis is $O(NM)$.

Among the LiRPA variants, IBP \rightarrow backward with a complexity of $O(D_y N)$ is usually the most efficient for classification models. To obtain tighter bounds for intermediate nodes which can also tighten the final output bounds, we may use pure forward or forward \rightarrow backward perturbation analysis with a complexity of $O(D_x N)$ which is usually larger than that of IBP \rightarrow backward when $D_y \ll D_x$. Since usually $D_y \ll D_x \ll M$, the pure backward perturbation analysis is much less efficient and thus can hardly scale to relatively large models.

D The GetDegree Auxiliary Function in Backward Mode Perturbation Analysis

Algorithm 3 Auxiliary Function for Computing Degrees

```

function GetDegree ( $v_k$ )
  New queue and  $Q.push(v_k)$ 
   $d_i \leftarrow 0$  ( $\forall i \leq n$ )
  while  $Q$  is not empty do
     $v_i = Q.head$ 
     $Q.pop()$ 
    for  $1 \leq j \leq m_i$  do
       $d_{u_{i,j}} \leftarrow d_{u_{i,j}} + 1$ 
      if  $u_{i,j}$  has not been in  $Q$  then
         $Q.push(v_{u_{i,j}})$ 

```

As mentioned in Section 3.4, we have an auxiliary “GetDegree” function for computing the degree d_i of each node v_i , which is defined as the the number of outputs nodes of v_i that the current node being bounded v_k is dependent on. This function is illustrated in Algorithm 3. We use a BFS pass. At the beginning, v_k itself is first added into the queue. Next, each time we pick a node v_i from the head of the queue, and v_k is dependent on v_i , and thus we increase each $d_{u_{i,j}} (1 \leq j \leq m_i)$ by one. v_k is also dependent on each $u_{i,j}$, and thus we also add $u_{i,j}$ to the queue if it has never been in the queue yet. We repeat this process until the queue becomes empty, and at this time any v_i that v_k is dependent on has been visited and has contributed to the $d_{u_{i,j}}$ of its input nodes. In this way, we are able to compute the degree of each node and can then proceed to propagating linear bounds in the backward manner as described in Section 3.4.

E Details of the Perturbation Space for Synonym-Based Word Substitution

For the perturbation specification defined on synonym-based word substitution, each word w has a substitution set $\mathbb{S}(w)$, such that the actual input word $w' \in \{w\} \cup \mathbb{S}(w)$. We adopt the approach for constructing substitution sets used by Jia et al. (2019). For a word w in a input sentence, Jia et al. (2019) first follow Alzantot et al. (2018) to find the nearest 8 neighbors of w in a counter-fitted word embedding space where synonyms are generally close while antonyms are generally far apart. They then apply a language model to only retain substitution words that the log-likelihood of the sentence after word substitution does not decrease by more than 5.0, which is also similar to the approach by Alzantot et al. (2018). We reuse the open-source code by Jia et al. (2019)¹ to pre-compute the substitution sets of words in all the examples. Note that although we use the same approach for constructing the lists of substitution words as Jia et al. (2019), our perturbation

¹<https://bit.ly/2KVxIFN>

space is still different from theirs, because we follow Huang et al. (2019) and set a small budget δ that limits the maximum number of words that can be replaced at the same time, which appears to be more realistic than allowing all the words to be replaced simultaneously.

F Details of the Models for Sentiment Classification and Their Certified Robust Training

We use two models in the experiments for sentiment classification: Transformer and LSTM. For Transformer, we use a one-layer model, with 4 attention heads, a hidden size of 64, and ReLU activations for feed-forward layers. Following Shi et al. (2020), we also remove the variance related terms in layer normalization, which can make Transformer easier to be verified while keeping comparable clean accuracies. For the LSTM, we use a one-layer bidirectional model, with a hidden size of 64. The vocabulary is built from the training data and includes all the words that appear for at least twice. Input tokens to the models are truncated to no longer than 32.

In the certified robust training, we use our algorithm to compute the certified upper bound of cross entropy loss when the input is perturbed within the corresponding perturbation space, and this loss is regarded as the robust loss. We combine the robust loss with a normal cross entropy loss following Jia et al. (2019), as

$$\min_{\theta} \mathbb{E}_{\mathbf{X} \in \mathbb{D}} [(1 - \kappa)\mathcal{L}(h(\mathbf{X}, \epsilon = 0); y; \theta) + \kappa\mathcal{L}(\bar{h}(\mathbf{X}, \epsilon); y; \theta),]$$

where we fix κ to 0.8 as Jia et al. (2019). ϵ is an hyperparameter to manually shrink the bounds of independent nodes during the warmup stage of certified robust training, which makes the objective easier to be optimized (Gowal et al., 2018; Jia et al., 2019). For independent node v_i , we shrink its concretized bounds and linear bounds:

$$\begin{aligned} \underline{h}_i &\leftarrow h_i(\mathbf{X}) - \epsilon(h_i(\mathbf{X}) - \underline{h}_i), \\ \bar{h}_i &\leftarrow h_i(\mathbf{X}) + \epsilon(\bar{h}_i - h_i(\mathbf{X})), \\ \underline{\mathbf{A}}^{(i)} &\leftarrow \epsilon \underline{\mathbf{A}}^{(i)}, \quad \bar{\mathbf{A}}^{(i)} \leftarrow \epsilon \bar{\mathbf{A}}^{(i)}, \\ \underline{\mathbf{b}}^{(i)} &\leftarrow \epsilon \underline{\mathbf{b}}^{(i)} + (1 - \epsilon)h_i(\mathbf{X}) \\ \bar{\mathbf{b}}^{(i)} &\leftarrow \epsilon \bar{\mathbf{b}}^{(i)} + (1 - \epsilon)h_i(\mathbf{X}). \end{aligned}$$

When training with IBP \rightarrow backward, ϵ is linearly increased from 0 to 1 during the first epoch, and is fixed to 1 in later epochs. When training with pure IBP, we spend 5 epochs for Transformer and 10 epochs for LSTM to linearly increase ϵ from 0 to 1, since pure IBP produces looser bounds and needs a longer warmup stage.

The models are trained using Adam optimizer (Kingma & Ba, 2014), and the learning rate is set to 10^{-4} for Transformer and 10^{-3} for LSTM. For LSTM, we also use gradient clipping with a maximum norm of 5.0.

G Details of IBP for Synonym-Based Word Substitution Perturbation Specification

In our experiments, we adopt the IBP for the perturbation specification of synonym-based word substitution (Jia et al., 2019; Huang et al., 2019) as a baseline. IBP is also used in our IBP \rightarrow backward perturbation analysis to compute bounds for intermediate nodes. IBP (Gowal et al., 2018) computes a lower bound and an upper bound for each neuron and these bounds are represented with concretized values. To apply it to word substitution perturbation constrained by a budget δ , we follow Huang et al. (2019). For a word sequence w_1, w_2, \dots, w_l , we construct a convex hull for the input node v_1 . We consider the perturbation of each word w_i , and for each possible $\hat{w}_i \in \{w_i\} \cup \mathbb{S}(w_i)$, we add vector

$$[e(w_{1\dots i-1}); e(w_i) + \delta(e(\hat{w}_i) - e(w_i)); e(w_{i+1\dots l})]$$

to the convex hull. The convex hull is an over-estimation of the value of v_1 . Next, for each direct output node of v_1 , denoted as v_i , we enumerate all the values in the convex hull and compute a corresponding output

value, and we take the element-wise minimum and maximum respectively as the concretized bounds of v_i . Regular IBP can then be performed after this concretization. In our framework, this modification of IBP is implemented when defining the perturbation specification and the operations of all possible output nodes of v_1 . Therefore, it is compatible with our general perturbation analysis framework.

H Supplementary Weight Perturbation Results

We perform an experiment to perturb weights by maximizing the natural cross entropy loss on test data with 10 steps and restrict the ℓ_∞ -norm of gradients with a given ϵ . The results are shown in Figure 6. As we can see, by increasing ϵ , the certifiably trained model achieves much better test accuracy and cross entropy loss than the naturally trained model.

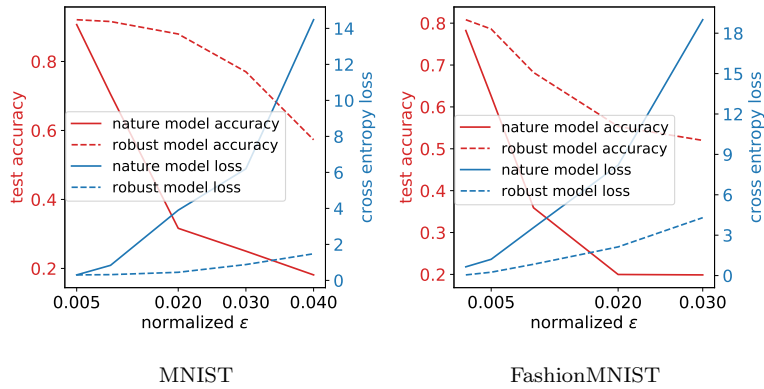


Figure 6: Test accuracy and loss on MNIST and FashionMNIST dataset by ℓ_∞ weight perturbation.